Computational and Structural Biotechnology Journal 19 (2021) 6328–6342

COMPUTATIONAL AND STRUCTURAL BIOTECHNOLOGY JOURNAL

journal homepage: www.elsevier.com/locate/csbj

The bone-degrading enzyme machinery: From multi-component understanding to the treatment of residues from the meat industry

Laura Fernandez-Lopez [a,1], Sergio Sanchez-Carrillo [a,1], Antonio García-Moyano [b,1], Erik Borchert [c,*,1], David Almendral [a], Sandra Alonso [a], Isabel Cea-Rama [d], Noa Miguez [a], Øivind Larsen [b], Johannes Werner [e], Kira S. Makarova [f], Francisco J. Plou [a], Thomas G. Dahlgren [b], Julia Sanz-Aparicio [d], Ute Hentschel [c,g], Gro Elin Kjæreng Bjerga [b], Manuel Ferrer [a,*]

[a] CSIC, Institute of Catalysis, 28049 Madrid, Spain
[b] NORCE Norwegian Research Centre, P.O. Box 22 Nygårdstangen, 5838 Bergen, Norway
[c] GEOMAR Helmholtz Centre for Ocean Research, 24148 Kiel, Germany
[d] Institute of Physical Chemistry "Rocasolano", CSIC, 28006 Madrid, Spain
[e] High Performance and Cloud Computing Group, Zentrum für Datenverarbeitung (ZDV), Eberhard Karls University of Tübingen, 72074 Tübingen, Germany
[f] National Center for Biotechnology Information, National Library of Medicine, National Institutes of Health, Bethesda, 20892 MD, USA
[g] Christian-Albrechts University of Kiel, 24118 Kiel, Germany

ARTICLE INFO

Article history:
Received 8 July 2021
Received in revised form 17 November 2021
Accepted 17 November 2021
Available online 23 November 2021

Keywords:
Bone microbiome
Bone degradation
Collagenase
Glycosidase
Metagenomics
Osedax mucofloris

ABSTRACT

Many microorganisms feed on the tissue and recalcitrant bone materials from dead animals, however little is known about the collaborative effort and characteristics of their enzymes. In this study, microbial metagenomes from symbionts of the marine bone-dwelling worm *Osedax mucofloris*, and from microbial biofilms growing on experimentally deployed bone surfaces were screened for specialized bone-degrading enzymes. A total of 2,043 taxonomically (closest match within 40 phyla) and functionally (1 proteolytic and 9 glycohydrolytic activities) diverse and non-redundant sequences (median pairwise identity of 23.6%) encoding such enzymes were retrieved. The taxonomic assignation and the median identity of 72.2% to homologous proteins reflect microbial and functional novelty associated to a specialized bone-degrading marine community. Binning suggests that only one generalist hosting all ten targeted activities, working in synergy with multiple specialists hosting a few or individual activities. Collagenases were the most abundant enzyme class, representing 48% of the total hits. A total of 47 diverse enzymes, representing 8 hydrolytic activities, were produced in *Escherichia coli*, whereof 13 were soluble and active. The biochemical analyses revealed a wide range of optimal pH (4.0–7.0), optimal temperature (5–65 °C), and of accepted substrates, specific to each microbial enzyme. This versatility may contribute to a high environmental plasticity of bone-degrading marine consortia that can be confronted to diverse habitats and bone materials. Through bone-meal degradation tests, we further demonstrated

Abbreviations: COLL, collagenases (peptidases families U32 and M9); DNS, dinitrosalicylic acid; FALGPA, N-[3-(2-furyl)acryloyl]-L-leucyl-glycyl-L-prolyl-L-alanine; HPAEC-PAD, High performance anion-exchange chromatography with pulsed amperometric detection; HEPES, 4-(2-hydroxyethyl)-1-piperazineethanesulfonic acid; HMM, Hidden Markov Models; MAG, Metagenome Assembled Genome; Neu5Ac-GM_2, N-acetyl-galactose-β-1,4-[N-acetylneuraminidate-α-2,3-]-galactose-β-1,4-glucose-α-ceramide; Neu5Ac-GM_3, Neu5Acα2-3Galβ1-4Glcβ1-ceramide; Ni-NTA, nickel-nitrilotriacetic acid; PEPT, peptidase (families S1, S8, S53, M61); *p*NP-NAβGal, *p*NP-N-acetyl-β-galactosaminide; *p*NP-NAβGlu, *p*NP-N-acetyl-β-glucosaminide; *p*NP-Neu5Ac, 2-O-(*p*-nitrophenyl)-α-acetylneuraminic acid; *p*NP-sugars, *p*-nitrophenyl-sugars; *p*NP-αAFur, *p*NP-α-arabinofuranoside; *p*NP-αAPyr, *p*NP-α-arabinopyranoside; *p*NP-αFuc, *p*NP-α-fucopyranoside; *p*NP-αGal, *p*NP-α-galactopyranoside; *p*NP-αGlu, *p*NP-α-glucopyranoside; *p*NP-αMal, *p*NP-α-maltoside; *p*NP-αMan, *p*NP-α-mannopyranoside; *p*NP-αRham, *p*NP-α-rhamnopyranoside; *p*NP-αXyl, *p*NP-α-xylopyranoside; *p*NP-βAPyr, *p*NP-β-arabinopyranoside; *p*NP-βCel, *p*NP-β-cellobioside; *p*NP-βFuc, *p*NP-β-fucopyranoside; *p*NP-βGal, *p*NP-β-galactopyranoside; *p*NP-βGlu, *p*NP-β-glucopyranoside; *p*NP-βGlucur, *p*NP-β-glucuronide; *p*NP-βLac, *p*NP-β-lactoside; *p*NP-βMan, *p*NP-β-mannopyranoside; *p*NP-βXyl, *p*NP-β-xylopyranoside; RHAM, α-rhamnosidases; SIAL, sialidases; αFUC, α-fucosidases; αGAL, α-galactosidases; αMAN, α-mannosidases; αNAG, α-N-acetyl-hexosaminidases; βGAL, β-galactosidases; βGLU, β-glucosidases; βNAG, β-N-acetyl-hexosaminidases.

* Corresponding authors at: GEOMAR Helmholtz Centre for Ocean Research, Wischhofstraße 1-3, 24148 Kiel, Germany (E. Borchert). Institute of Catalysis, CSIC, Marie Curie 2, 28049 Madrid, Spain (M. Ferrer).

E-mail addresses: eborchert@geomar.de (E. Borchert), mferrer@icp.csic.es (M. Ferrer).

[1] These authors contributed equally to this work.

https://doi.org/10.1016/j.csbj.2021.11.027

that some of these enzymes, particularly those from *Flavobacteriaceae* and *Marinifilaceae*, may be an asset for development of new value chains in the biorefinery industry.

1. Introduction

Bone biodegradation in terrestrial and marine environments has been and is of great interest in the archaeological sector. For example, the degree of preservation of bones has been associated, in some cases, with the presence of microorganisms capable of degrading them [1,2]. A recent study has also demonstrated the impact of bacterial colonization in animal bone health and bone loss [3], and therefore, its composition must be considered during microbiota reconstitution trials. Despite the impact that microorganisms can have in the archaeological and health sectors, their relevance in the biotechnological sector needs to be highlighted. Indeed, meat production will be financially hit by carbon tax and other measures to reduce consumption as a way to limit methane/CO_2 release and climate change [4,5]. This is why refinement processes are being increasingly developed with meat/bone-waste streams to increase revenue by, for example, producing hydrolysates with blood pressure lowering [6] and antihypertensive [7] properties, as well as peptide- and lipid-enriched hydrolysates useful in microbiological media [6] and human consumption [8]. However, the breakthrough in the degradation of bones is impaired by the lack of efficient enzymes to degrade the heterogeneous and dense phases within bone tissue [9–12]: a mineral phase (hydroxyapatite crystals), water, and an organic phase that includes proteins such as collagen (90% of the protein content) and structural glycoproteins (e.g., containing mannose, galactose, amino hexose sugars and sialic acid), and lipids such as cholesterol. Among these components, the most recalcitrant is collagen. While there are numerous microorganisms in the soil and marine sediments that produce collagenases, none have ever been demonstrated to degrade mineralized collagen, because the bond between hydroxyapatite and collagen is at the molecular level [12]. Even the active sites of collagenases produced by microorganisms and osteoclasts cannot access collagen and therefore they must secrete acids to demineralise the crystalline structure first, before collagenases can act [13]. Streamlining discovery of enzymes capable of degrading bone materials, from the most recalcitrant components such as collagen to those that attack the intricate polysaccharides and polypeptide framework, is thus of considerable interest.

The discovery of such enzymes can principally be achieved by selectively prospecting enzymes encoded by genes of non-cultivable soil and marine microorganisms, in combination with methodological advancements and characterization efforts. Two relevant such sources are the microbial biofilms that develop on the surface of bones from shallow and deep water marine environments, and the symbionts of bone-dwelling worms, e.g., *Osedax mucofloris*. These bio-resources have been shown to have a wide microbial diversity, whose compositions and involvement in the various and successive events involved in the degradation of mature bone, have been investigated to some detail [14–27]. In this process, recent metagenome sequence analyses suggested that, as mentioned above, the acidification by some organisms is key before the hydrolysis of bone matrix is initiated by other community members [27]. They all together produce a broad set of enzymes whose characteristics and biotechnological potential remains to be elucidated [28]. Indeed, the available biochemical knowledge is restricted to identification of peptidolytic/collagenolytic activity in *Osedax* tissues enriched in certain symbionts [19,29,30].

In this study, we asked the following questions: from an environmental point of view, how diverse and novel is the bone-degrading enzyme repertoire in marine bone-associated microbial consortia? From a technological point of view, do such enzymes have a potential for the emerging bio-based economy, in particular, for the valorisation of bone residues from the meat processing industry? To answer these questions, herein we established a multi-disciplinary approach that includes I) field experiments in combination with metagenomics and targeted screening for microbial enzymes with proteolytic/collagenolytic and glycohydrolytic activity, II) gene synthesis, heterologous protein expression and detailed biochemical and structural characterization, and III) pre-industrial trials on bone meal degradation using enzyme cocktails. Altogether, this study deepens into the diversity and presumptive microbial interactions to promote bone degradation in marine bone-associated microbiomes, and their use as potential biological resources for highly versatile and performance hydrolytic enzymes whose potential for bone biorefinery process is also evaluated.

2. Materials and methods

2.1. Source and profiling of enzymes and taxonomic assignation

In this study we used a curated database with diverse protein sequences featuring enzyme families relevant to bone degradation to identify by homology BLAST-search similar sequences in Metagenome Assembled Genomes (MAGs) and contigs not binned as MAGs from marine bone associated microbiomes [27]. The sequences encoding targeted bone-degrading enzymes were selected by HMM [27] and DIAMOND [31]. The tools were applied to raw sequencing reads deposited in the sequence read archive (SRA) of NCBI under the BioProject ID PRJNA606180 and with the BioSample accession numbers given in Table 1. In both cases, a custom database containing 17,072 taxonomically diverse protein sequences, representing ten key enzyme families targeting bone components [27] were used (see details in Table S1). For HMM based searches, multiple alignments of each enzyme family were generated with ClustalW version 2.1 [32] and HMMER version 3.1b1 [33] was employed to construct the models for each family with *hmmbuild* and *hmmsearch* to search, keeping those with a bit-score greater than or equal to 100 [27]. For DIAMOND searches, *blastp* with default parameters was used, selecting the best match (percent identity $\geq$ 60%; alignment length $\geq$ 70; e-value $\geq 1e^{-5}$). Taxonomic affiliation of candidate sequences was performed as described by Borchert et al. [27] as well as by MetaErg version 1.2.1 [34].

2.2. Chemicals

Fetuin from fetal bovine serum, 3′-sialyllactose, 6′-sialyllactose, galactose-α-1,3-galactose globotriaosylceramide, globotriaosylsphingosine, Neu5Ac-GM_2, Neu5Ac-GM_3, acetylchitobiose, acetylchitotriose, acetylchitotetraose, N-[3-(2-furyl)acryloyl]-L-leucyl-glycyl-L-prolyl-L-alanine (FALGPA), *p*NP-αAFur, *p*NP-αAPyr,

Table 1
Samples, sequencing statistics and bone metagenome size.

ID[1]	Bone type[2]	Collection date (dd.mm.yyyy)	Assembly size (Mbp)	Nr. of bone-degrading enzymes[3]	Frequency[4]	BioSample[5]
OB_{C0}	Cow (tibia)	08.01.2017	263.32	15	0.057	SAMN14086996
OB_{S0}	Sheep (lower leg)	08.01.2017	343.32	154	0.45	SAMN14086997
OB_{T0}	Turkey (femur)	08.01.2017	375.17	241	0.64	SAMN14086998
OB_{T1}	Turkey (femur)	08.02.2017	303.49	34	0.11	SAMN14087000
OB_{T2}	Turkey (femur)	14.04.2017	228.14	6	0.026	SAMN14087003
BB_{T0}	Turkey (femur)	27.01.2017	1028.74	776	0.75	SAMN14087007
BB_{T1}	Turkey (femur)	08.02.2017	349.28	300	0.86	SAMN14087005
BB_{T2}	Turkey (femur)	11.12.2017	453.81	170	0.37	SAMN14087006
BB_{C0}	Cow (tibia)	11.01.2017	549.12	345	0.63	SAMN14087008

[1] OB_{C0}, BB_{C0}, OB_{S0} and OB_{T0} were obtained as follows: Turkey thigh bones, and sheep and cow lower leg bones were deposited in Byfjorden (60,238185N, 5,181210E) outside Bergen, Norway at a depth of 68 m in May 2016, incubated for nine months and retrieved using a small ROV throughout 2017. Microbial mats were scrapped off the bone surfaces and *O. mucofloris* worms dissected, and *O. mucofloris*-associated Bone symbiotic microbiomes from Cow (OB_{C0}), Sheep (OB_{S0}) and Turkey bones (OB_{T0}), as well as Bone surface-associated Biofilms (BB) microbiomes from Cow lower leg bones (BB_{C0}), were isolated and sequenced, and reads quality-filtered and assembled to generate non-redundant metasequences, as previously described [27]. OB_{T1} and BB_{T1} were obtained as follows: OB and BB microbiomes from turkey thigh bones that after nine months deposited in Byfjorden were further maintained in aquaria for one (OB_{T1} and BB_{T1}) and three (OB_{T2} and BB_{T2}) months, were processed as before. Note: samples OB_{T0}, OB_{T1}, OB_{T2}, BB_{T0}, BB_{T1}, BB_{T2}, and BB_{C0} were referred to as samples A5, A9, B4, I1, D1, D2 and I3, respectively, in Borchert et al. [27]. Samples OB_{C0} and OB_{S0} are herein reported for first time.
[2] Cow: *Bos taurus*; Turkey: *Meleagris gallopavo*; Sheep: *Ovis aries*.
[3] As identified in the microbiomes by HMM and DIAMOND searches.
[4] Frequency corresponds to the nr. of candidate hits per Mbp.
[5] BioProject nr. PRJNA606180.

*p*NP-βAPyr, *p*NP-βCel, *p*NP-αFuc, *p*NP-βFuc, *p*NP-αGal, *p*NP-βGal, *p*NP-αGlu, *p*NP-βGlu, *p*NP-βGlucur, *p*NP-βLac, *p*NP-αMal, *p*NP-αMan, *p*NP-βMan, *p*NP-NAβGal, *p*NP-NAβGlu, *p*NP-Neu5Ac, *p*NP-αRham, *p*NP-αXyl, and *p*NP-βXyl, were ordered from Merck Life Science S.L.U., (Madrid, Spain). Prior to use, all these chemicals were solubilized in dimethylsulfoxide (DMSO) to prepare a 10 mg ml^{-1} stock solution. Note: all sugar-based substrates were tested for all enzymes herein characterized, and only for those for which activity was observed, biochemical parameters were determined.

2.3. Enzyme selection, production and purification

For selecting gene sequences most likely encoding full-length enzymes to be further synthesized, the following protocol was applied: i) bioinformatically-selected with CD-HIT [35] sequences from Table S2 with a percentage of identity over 90% are removed, keeping the longest, to avoid redundancy; ii) sequences with a length below the median length of its family in the custom database were removed; iii) sequences are analyzed by BLAST [36] as well as homology modeling programs Swissmodel [37] and Phyre2 [38] to identify those encoding full-length enzymes containing all domain composition; iv) taxonomic affiliation is also considered for covering a broader diversity; v) the presence of a predicted signal peptide (according to signalP v5.0) for extracellular export is also taken as a positive feature. In total, 47 enzymes were selected for further expression.

The 47 selected sequences were synthesized as codon-optimized DNA from Twist Biosciences (San Francisco, US), with flanking inward-oriented SapI sites for directional fragment exchange (FX) cloning. Leader sequences were omitted from the final gene construct, allowing proteins to be expressed intracellularly. The synthetic ORFs (T0182 to T0228) were delivered in a propagation plasmid, which was directly used as entry plasmid in parallel FX cloning [39] into two different plasmids (p1 and p12) that supply different solubility and affinity tags for expression in *E. coli* [40], namely, N- or C-terminally histidine (his) tagged proteins, respectively. The soluble His-tagged proteins were produced at 16 °C (or 12 °C in case of T0182) in Luria-Bertani (LB) medium (10 g l^{-1} tryptone, 10 g 1^{-1} NaCl, 5 g 1^{-1} yeast extract) supplemented with 100 μg ml^{-1} ampicillin, and purified at 4 °C after binding to a Ni-NTA His-Bind resin (Merck Life Science S.L.U., Madrid, Spain) as described [41]. The purity was assessed as > 98% using SDS-PAGE analysis in a Mini PROTEAN electrophoresis system (Bio-Rad, Madrid, Spain). Purified protein was stored at −86 °C until use at a concentration of 10 mg ml^{-1} in 40 mM 4-(2-hydroxyethyl)-1-piperazineethanesulfonic acid (HEPES) buffer (pH 7.0). A total of about 0.5–32 mg total purified recombinant proteins were obtained from 1-liter culture, depending on the protein.

2.4. Determination of substrate specificity, and kinetic and optimal parameters of glycosidases

Hydrolytic activity towards the 21 *p*NP-sugars described in Section 2.2 was performed, for all enzymes, in 96-well plates in a Synergy HT Multi-Mode Microplate Reader in continuous mode at 348 nm (isosbestic point *p*-nitrophenol, ε = 4,147 M^{-1} cm^{-1}) over 30 min, and the absorbance per minute was determined from the slopes generated, as previously described [42]. One unit (U) of enzyme activity was defined as the amount of enzyme required to transform 1 μmol of substrate in 1 min under the assay conditions using the reported extinction coefficient. Unless otherwise indicated, for K_m and V_{max} determination - [protein]: 1–50 μg ml^{-1}, depending on the protein; [substrate]: 0–14 mM; reaction volume: 200 μl; T (Temperature): 30 °C; pH: 7.0 (50 mM Britton and Robinson buffer); time: 30 min. For k_{cat} determination – [protein]: 0–0.4 mg ml^{-1}; [substrate]: 10 mM; reaction volume: 200 μl; T: 30 °C; pH: 7.0 (50 mM Britton and Robinson buffer); time: 30 min.

Hydrolytic activity towards fetuin, 3′-sialyllactose, 6′-sialyllactose, Neu5Ac-GM_2 and Neu5Ac-GM_3, galactose-α-1,3-galactose, globotriaosylceramide, and globotriaosylsphingosine was determined as follows. A volume of 2 μl of a stock substrate solution (10 mg ml^{-1} in DMSO) was added to 196 μl of 50 mM Britton and Robinson buffer, pH 7.0. Then, 2 μl of protein (from a 10 mg ml^{-1} in 40 mM HEPES buffer pH 7.0) were immediately added. The total reaction volume was 200 μl and the temperature set at 30 °C, for a total time of 24 h. Oligosaccharides were analyzed by High Performance Anion-Exchange Chromatography with Pulsed Amperometric Detection (HPAEC-PAD) (see Section 2.8).

For optimal pH determination of glycosidases [protein]: 0.002–0.04 mg ml^{-1} (stock solution: 10 mg ml^{-1}, 40 mM HEPES pH 7.0), depending on the protein; [substrate]: 0.3 mg ml^{-1} (stock: 10 mg ml^{-1}, DMSO); buffer: 50 mM Britton and Robinson buffer, pH 3.0–8.5; volume: 200 μl; T: 30 °C; time: 30 min. For optimal temperature determination of glycosidases [protein]: 0.002–0.04 mg ml^{-1} (stock: 10 mg ml^{-1}), depending on the protein; [sub-

strate]: 0.3 mg ml^{-1} (stock: 10 mg ml^{-1}); buffer: 50 mM Britton and Robinson buffer, pH 7.0; volume: 200 μl; T: 5–85 °C; time: 30 min. For pH and temperature determinations, substrates with best transformation rates were used.

All assays were performed in triplicate, and values were corrected for non-enzymatic transformation.

2.5. Characterization of collagenases

The collagenase assay was based on the ability of peptidases to hydrolyse fluorescent-labelled casein as described by Thompson et al. [43]. Briefly, the substrate used was a green fluorescent-labelled (BODIPY-FL) casein (Molecular Probes, #E6638) and the working solutions were all prepared and assay conditions performed, as recommended by the provider, with small modifications. Briefly, 100 μl of BODIPY-FL casein stock solution (10 μg ml^{-1}) was added to each well in a 96-microtitre plate and subsequently topped with 90 μl of the 50 mM Britton and Robinson buffer, pH 3.0–8.5. The plate was temperature equilibrated in an oven at the particular assay temperature for 3 min covered with an adhesive foil to limit evaporation. The plate was then placed in fluorescence plate reader before adding 10 μl of the enzyme preparation solution (10 mg ml^{-1}) to each microtitre plate well with the use of a multichannel pipette. The fluorescence readings in all wells were measured immediately after the plate was gently shaken for 3 s. The rate of hydrolysis in each assay was recorded at 15 s intervals over 20 min. Measurements were carried out using a fluorescence plate reader (Synergy HT Multi-Mode Microplate Reader). The assays were performed for each pH (3.0–8.5, using 50 mM Britton and Robinson buffer) at 30 °C and temperature ranging from 5 to 80 °C, at pH 7.0 (using 50 mM Britton and Robinson buffer). The fluorescence readings for the reaction steady state (within the first minute of the assay) were used to generate a progress curve (arbitrary fluorescence unit vs. time) from which a line slope value was determined. Enzyme unit was calculated as described by Lee et al. [44]. All assays were performed in triplicate, and values were corrected for non-enzymatic transformation.

Collagenase activity was also measured using FALGPA. Enzyme assays, in triplicates, were performed as detailed in the manufacture's protocol (Merck Life Science S.L.U., Madrid, Spain). Unless otherwise indicated, for K_m determination – [protein]: 1 mg ml^{-1}; [substrate]: 0–10 mM; reaction volume: 200 μl; T: 30 °C; pH: 7.0 (50 mM Britton and Robinson buffer); time: 30 min. For k_{cat} determination – [protein]: 0–0.4 mg ml^{-1}; [substrate]: 10 mM; reaction volume: 200 μl; T: 30 °C; pH: 7.0 (50 mM Britton and Robinson buffer); time: 30 min. Absorbance was monitored at 324 nm (ε of 2,250 mM^{-1} cm^{-1}). One unit was defined as the amount of enzyme required to hydrolyse 1 mmol FALGPA in 1 min under the indicated assay condition.

2.6. Chromogenic bone-meal degradation tests

Bone meal (Weibulls, Sweden) was purchased from a local nursery and rendered chromogenic by GlycoSpot (Søborg, Denmark) as described previously [45]. Prior to the assays, the working solutions were all prepared and assay conditions performed, as recommended by GlycoSpot. Two hundred microlitres of 50 mM Britton and Robinson buffer, pH 7.0, were added to each of wells. The plate was then placed in a Synergy HT Multi-Mode Microplate Reader to equilibrate to 30 °C. Thereafter 10 μl of the enzyme solutions were added to each microtitre plate well using a multichannel pipette and the absorbance readings in all wells were measured immediately after the plate was gently shaken for 3 s. The enzyme solutions consist of: I) 10 mg ml^{-1} purified T0182; II) 10 mg ml^{-1} of each of the T0193, T0199, T0204, T0207, T0209, T0215, and T0216 purified proteins (herein after referred as glycohydrolytic *cocktail*); III) 10 mg ml^{-1} purified T0182 and all proteins constituting the glycohydrolytic *cocktail*; and VI) buffer without protein (control sample). The absorbance readings at 517 nm for the reaction steady state (within the first 20 s of the assay) were used to generate a progress curve (arbitrary fluorescence units vs. time) from which a line slope value was determined. Enzyme unit was calculated as Δ absorbance per min. All assays were performed in triplicates, and values were corrected for non-enzymatic transformation.

2.7. Chicken thigh bone degradation tests

Chicken thigh bone, sourced from a local butcher shop, was used for additional degradation tests. The bone (about 12 g) was demineralized by immersion in a test tube containing 120 ml of 3 M HCl solution (Merck Life Science S.L.U., Madrid, Spain). After overnight incubation at room temperature, the bone was removed and washed extensively with distilled water. The demineralized bone, which now had turned elastic, was then cleaned to remove non-collagenous proteins and then freeze dried in liquid nitrogen, lyophilized to fully eliminate the water, and finally pulverized with a coffee grinder (Moulinex Super Junior S). For the degradation test a protocol commonly employed for preparation of sugar-polymers for biomass degradation tests, was adapted [46]. Briefly, 1 g of pulverized dry bone material thus obtained was added to a 100 ml Erlenmeyer flask containing 60 ml pre-warmed buffer (50 mM Britton and Robinson buffer, pH 7.0) at 60 °C. The mixture was kept overnight at 60 °C under agitation with a magnetic stirrer, after which 40 ml of the same buffer was added, to achieve a final substrate concentration of 1% (w/v). For the tests, 20 μl of the enzyme solutions (10 mg ml^{-1}), were added to 480 μl bone solution prepared as above, in a 1.5 ml Eppendorf. The enzyme solutions tested were the I)-IV) described in Section 2.6. The reactions, done in triplicates, were kept at 30 °C at 900 rpm in a thermal block. Degradation level was followed by measuring the concentration of reducing sugars released by the dinitrosalicylic acid (DNS) method adapted to a 96-well microplate scale [47] and the degradation products profile by HPAEC-PAD (see Section 2.8).

2.8. HPAEC-PAD analysis

Sample aliquots (300 μl) were firstly mixed with absolute ethanol until the final ethanol concentration was 70% in order to precipitate protein material. They were subsequently centrifuged (10000 *g*, 5 min) and filtered with 0.45 μm nylon filters (Cosela, Sevilla, Spain). Then, the samples were desiccated with a vacuum concentrator 5301 (Eppendorf) at 30 °C, and 200 μl of filtered aqueous solution were added for the analysis by HPAEC-PAD. The analysis was carried out at 30 °C by HPAEC-PAD, Dionex ICS3000 system (Sunnyvale, CA, USA), an anion-exchange CarboPack PA-100 column (4 × 250 mm) connected to a CarboPac PA-100 guard column (4 × 50 mm), and an autosampler (model AS-HV). The initial mobile phase was 30 mM NaOH at 0.5 ml min^{-1} and a gradient from 30 to 60 mM NaOH was performed in 15 min. Then, a second gradient was carried out going from 60 to 120 mM NaOH and increasing sodium acetate until 64 mM in 35 min. In the next 10 min, sodium acetate was increased until 160 mM and NaOH was changed from 120 mM to 90 mM. In another 10 min, NaOH was increased from 90 mM to 110 mM and sodium acetate decreased until 96 mM. Finally, the mobile phase was changed back to the initial conditions (30 mM NaOH) in 1 min and maintained for 15 min. Eluents were degassed by flushing with helium and peaks were analyzed using Chromeleon software.

2.9. Three dimensional modeling

The analysis of the sequences performed using BLAST [36] allowed the identification of the domain composition within each protein. Models of each domain were built using the homology modeling programs Swissmodel [37] and Phyre2 [38]. From the different outcomes, the best-ranked models were selected for each protein to be presented in this work. PDB codes used as templates are shown in the results section.

3. Results and discussion

3.1. Selection of bone-degrading enzymes

We have recently established and manually curated a database with 17,072 taxonomically diverse protein sequences (Table S1) featuring ten key enzyme families, potentially targeting different bone matrix components [27]. They include enzymes covering one peptidolytic/collagenolytic [collagenases U32 (COG0826) and M9 (Pfam01752) and peptidases families S1 (COG0265), S8/S53 (and Pfam00082) and M61 (Pfam17899) peptidases] and nine glycohydrolytic [α-mannosidases (COG0383), α-sialidases (COG4409), α-fucosidases (COG3669), α-N-acetyl-hexosaminidases (pfam16499), β-N-acetyl-hexosaminidases (COG1472), α-galactosidase (Pfam16499), β-galactosidases (COG3250), α-rhamnosidases (Pfam17132), and β-glucosidase (COG1472)] activities.

A total of 733 candidate hits, homologous to the aforementioned families, were previously extracted by HMM profiling from 59 MAGs reconstructed from marine bone associated microbiomes retrieved from turkey and cow bone deployment field experiments, detailed in Table 1 [27]. In this study, the same protocol was applied to further search for additional candidate hits in contigs (>500 bp in length) not assembled as MAGs in this set of samples [27], as well as in contigs (>500 bp in length) from microbiomes newly retrieved from new field experiments with cow and sheep bones (see Table 1). As a complementary tool, DIAMOND [31] was applied (for parameters see Section 2.1) to all samples in Table 1.

A total of 1,301 additional candidate hits were retrieved, which together with those previously identified, make a total of 2,043 sequences, distributed among all 10 targeted families (Tables S2 and S3). A set of 1,977 of those hits were identified by HMM, while 338 by DIAMOND (Table S2). Only 272 (13.3%) were identified by both methods, demonstrating their complementary utility for enzyme search.

As summarized in Table S2, the 2,043 proteins exhibited amino acid sequence identities ranging from 28.6 to 100% to homologous proteins in the non-redundant (nr) NCBI database (calculated using DIAMOND) with a median value of 72.2% (23.4% interquartile range (IQR)). The pairwise global alignment (Needleman-Wunsch algorithm) percentage of identity for all sequences within each of the families ranged from 2.7 to 100%, with a median value of 23.6% (3.7% IQR). To conclude, the 2,043 hits consist of diverse and non-redundant protein sequences, distantly related in many cases to known homologues, as expected from a pecialized microbial community in the marine environment involved in degradation of bones.

3.2. Microbial source of bone-degrading enzymes

In this work we provide an understanding of how bone-associated marine microbes and enzymes presumptively function together to degrade bone material as a whole. The interest in this type of studies lies in the fact that marine microbial bone degradation has only been scarcely studied previously, most research focused on the degradation machinery of the bone-eating worm *Osedax* [13,15,23,29] and its bacterial endosymbionts, which are ultimately not directly involved in the degradation of bone components [19,30]. The biofilms developing independently from *Osedax* on the bone outside have been studied so far only with different DNA sequencing methods, but functional prove is lacking [21,25,28,48].

As shown in Table S2, a total of 45 enzymes could be assigned only at phylum level, 164 at class level, 386 at family level, 1,195 at genus level, and 93 remained as unclassified, according to the automated pipelines for annotating metagenome-assembled contigs described previously [27] and MetaErg [34]. By focusing at phylum level, the 1,949 enzymes potentially involved in bone degradation with unambiguous taxonomic assignation, affiliated to 40 phyla (Fig. 1). Members of the *Bacteroidota* were the only ones hosting all 10 targeted proteolytic/collagenolytic and glycohydrolytic activities and thus, they could potentially use recalcitrant bone material as a sole carbon source. Within it, only members of the families *Flavobacteriaceae* and *Marinifilaceae* (representing 53% of total *Bacteroidota* hits) hosted all 10 activities (Table S2). This is in consonance with their previous role assigned through the analysis of MAGs [27]. As shown in Fig. 1 and Table S2, members of other phyla significantly contributed also to the bone degradation by hosting 6–7 activities each: i) *Proteobacteria,* e.g., *Beggiatoaceae, Nitrincolaceae, Alteromonadaceae,* and *Kangiellaceae* representing 36% total hits; ii) *Chloroflexota,* e.g., *Anaerolineae* representing 95% total hits; iii) *Firmicutes*, e.g., *Paenibacillaceae* and *Clostridiaceae* representing 30% total hits; iv) *Campylobacterota,* e.g., *Sulfurimonadaceae*, *Sulfurospirillaceae, Sulfurovaceae,* and *Thiovulaceae* representing 83% total hits; v) *Verrucomicrobiota,* e.g., *Kiritimatiellae*, *Lentisphaeria* and *Verrucomicrobiae* representing 98% total hits; and vi) *Spirochaetota,* e.g., *Spirochaetaceae*, representing 61% total hits. In contrast, 21 bacterial phyla do show a high specialization, as they contributed with single hydrolytic activities.

At the functional level, peptidases (including U32 and M09 collagenases; [51]), α-mannosidases, β-glucosidases and β-galactosidases were the enzymes associated to or hosted by a higher number of taxonomically diverse microbes (29, 19, 16 and 14 phyla, respectively), followed by α-fucosidases (twelve phyla) and β-N-acetyl-hexosaminidases (nine phyla) (Fig. 1). In contrast, sialidases (three phyla), α-galactosidases (two phyla), α-N-acetyl-hexosaminidases (two phyla), and α-rhamnosidases (one phylum), were the ones associated to the fewest number of phyla.

The fact that members of 29 phyla produced peptidases, including U32 and M09 collagenases [51], and that they represent about 48% of the total hydrolytic enzymes identified (Tables S2 and S3), is consistent with the fact that around 30% of mature bone is composed of organic compounds, of which 90–95% is collagen [9–12]. Thus, given its abundance in mature bone, a massive proteolytic/-collagenolytic effort is required. Based on the data presented in Fig. 1 and Table S2, this effort is primarily driven by four members of the community that combined produced 92% of all U32 and M09 collagenolytic hydrolases: i) *Proteobacteria*, e.g., *Beggiatoaceae, Nitrincolaceae, Alteromonadaceae,* and *Kangiellaceae*, representing 43% of the hits, hosting both M09 and U32 collagenases; and ii) *Bacteroidota* (e.g., *Flavobacteriaceae* and *Marinifilaceae,* 63% hits), *Desulfobacterota* (e.g., *Desulfobacteraceae*, 61% hits) and *Campylobacterota* (e.g., *Sulfurimonadaceae*, *Sulfurospirillaceae, Sulfurovaceae,* and *Thiovulaceae,* 78% hits) hosting only U32 collagenases. The fact that different microbial members host different families of collagenases suggests they have different ways to attack the collagenolytic material, with *Proteobacteria* most likely contributing with a wider degradation capacity by hosting M09 and U32 families.

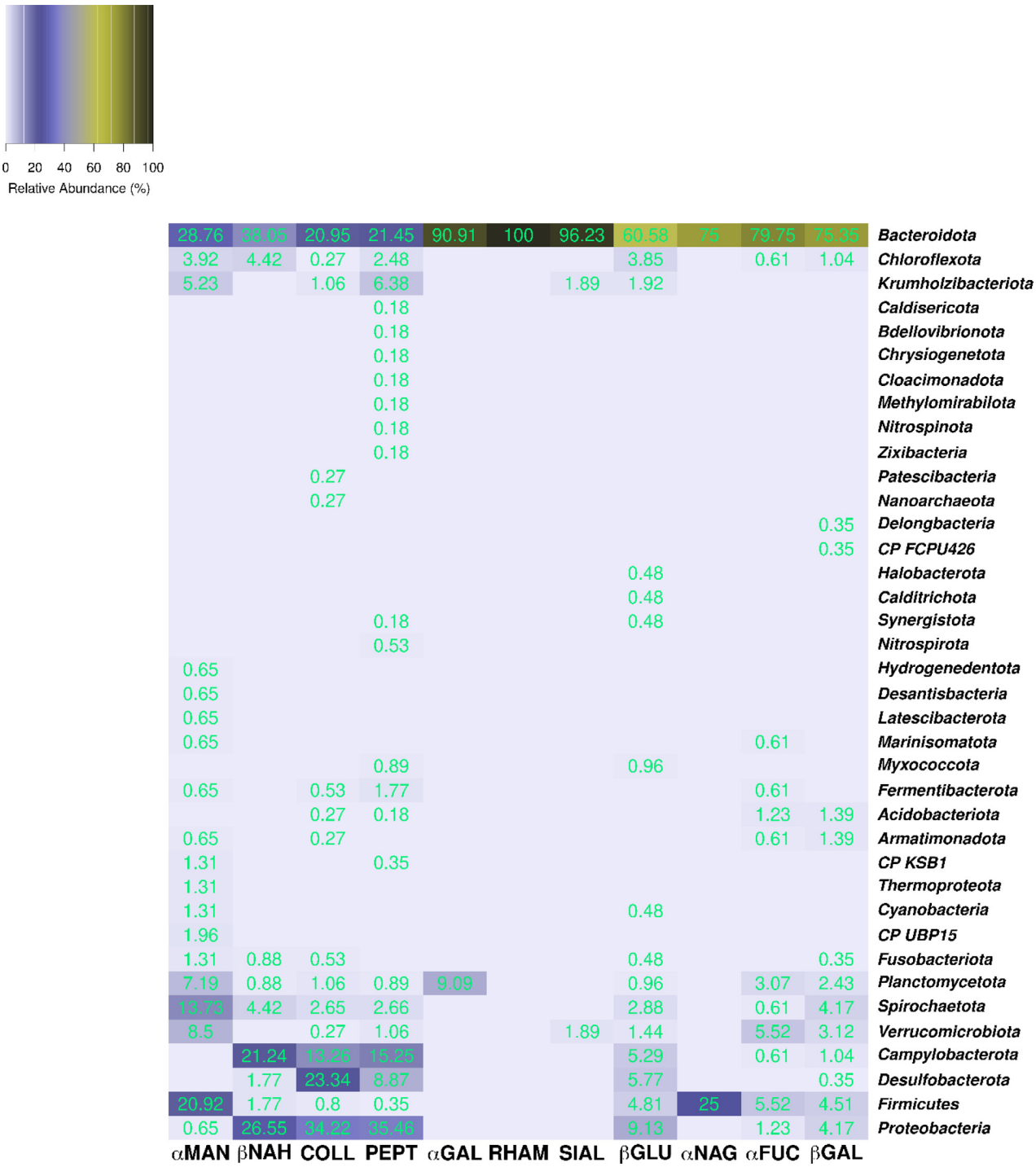

Fig. 1. Heatmap representing the relative abundance (%) of bone-hydrolytic enzymes per family assigned to different microorganisms at phylum level. Here, the data for all marine bone-associated microbiomes in Table 1 are shown. Values indicate the relative abundance level of enzymes, involved in the degradation of each bone component, binned to each taxonomic group. For abbreviations see abbreviation lists in page 1. The plot was made with gplot R package version 3.1.1 [49,50].

Bones also contain sialo/glycoproteins that confer recalcitrant character [11]. Based on taxonomic affiliations in Fig. 1 and Table S2, we hypothesized that the hydrolysis of sialoproteins will be driven by three members, namely, *Bacteroidota* (particularly, *Flavobacteriaceae* and *Marinifilaceae,* 51% hits), and to much lower extend *Verrucomicrobiota* (only one hit) and *Krumholzibacteriota* (only one hit), each containing a different set of sialidases.

A wide cooperation is suggested for the hydrolysis of glycoproteins, for which 7 phyla are the main contributors according to the relative abundance (%) of enzymes (Fig. 1): i) *Bacteroidota*, particularly *Flavobacteriaceae* and *Marinifilaceae* (51% hits), which host enzymes presumably degrading all targeted sugar components, including α-mannose, β-N-acetyl-hexosamine, α-galactose, α-rhamnose, β-glucose, α-N-acetyl-hexosamine, α-fucose, and β-galactose; ii) *Firmicutes,* e.g., *Paenibacillaceae* and *Clostridiaceae*, likely contributing to attack α-mannose and α-N-acetyl-hexosamine residues; iii) *Proteobacteria,* e.g., *Alteromonadaceae, Kangiellaceae* and *Nitrincolaceae*, likely contributing to degrade

β-N-acetyl-hexosamine and to less extend β-glucose and β-galactose; iv) *Planctomycetota,* likely contributing to degrade α-galactose and α-mannose; v) *Campylobacterota*, e.g., *Sulfurimonadaceae* and *Sulfurovaceae*, likely degrading β-N-acetyl-hexosamine and to less extend β-glucose; vi) *Spirochaetota*, e.g., *Spirochaetaceae,* likely degrading α-mannose; and vii) *Verrucomicrobiota,* e.g., *Victivallaceae*, likely degrading α-mannose. It is noteworthy that this contribution is based on the number of distinct enzymes assigned to each taxonomic group, although *in vivo* it may depend on the bacterial cell number, and the *in situ* expression level and performance of the enzymes assigned to each taxonomic group.

To conclude, in marine bone-associated microbial consortia an extensive functional redundancy among microorganisms potentially participating in bone degradation exists, as well as a high degree of functional specialization. Results also point to the relevant role of *Flavobacteriaceae* and *Marinifilaceae* as being generalists (i.e., multiple bone-degrading enzyme producers) in marine bone-associated microbiomes, in close cooperation with specialists enzyme producers that included at least *Alteromonadaceae, Anaerolineae, Clostridiaceae, Desulfobacteraceae, Kangiellaceae, Kiritimatiellae*, *Krumholzibacteriota, Lentisphaeria*, *Nitrincolaceae, Paenibacillaceae, Planctomycetota, Spirochaetaceae, Sulfurimonadaceae*, *Sulfurospirillaceae, Sulfurovaceae*, *Verrucomicrobiae,* and *Victivallaceae*. To date, no studies focusing on the taxonomic analysis of enzymes involved in bone degradation have been reported and it is therefore difficult to detail the extent to which these taxonomic groups and the enzymes they contain are different from those present in other environments and bones. That said, the bone degrading community herein reported significantly differs from those in femora or humeri of domestic swine [25], other defleshed bones [21] and whale fall [28] deposited or submerged in marine associated environments; metabarcoding revealed they are enriched in Firmicutes (e.g., families *Lachnosppiraceae* and *Clostridiaceae*), Bacteriodetes (e.g., family *Marinilabiaceae*), sulfate-reducing families of the phyla Fusobacteria (e.g., *Fusobacteriaceae*), Proteobacteria (e.g., *Pseudomonadaceae*, *Desulfovibrionaceae*, *Helicobacteraceae* and *Rhodobacteraceae*) and Thermotogae (e.g., *Thermotogaceae*). Although these differences may be due to different depositional environments, the results reflect functional novelty associated to a specialized bone-degrading marine community herein investigated.

Therefore, in this study we have expanded the range of microbial players involved in the bone degradation process in marine bone associated microbiomes, even compared to our previous study that gave a leading role only to *Bacteroidota* (*Flavobacteriaceae* and *Marinifiliaceae*) and γ-*Proteobacteria* (*Alteromonadaceae* and *Kangiellaceae*) [27]. It is worth mentioning that the capacity of these members to degrade polysaccharides and polypeptides like collagen, gelatin, agar, chitin, ulvan, alginate, carrageen, cellulose, xylan, elastin, spongin, or others are known [see ref. in 27], and here we have provided further evidences they may also be versatile degraders of other complex molecules including collagen and sialoproteins. Sulfur-metabolizing bacteria of *Desulfobacteraceae*, *Sulfurovaceae, Sulfurimonadaceae, Sulfurospirillaceae, Krumholzibacteriota* and *Spirochaetaceae* families have been suggested to mostly contribute bone degradation by promoting acidification [27], but their presumptive role in also contributing to the degradation of collagen and specific polysaccharides was first suggested in this study. Results highlight also that nitrogen metabolizing bacteria such as members of *Nitrincolaceae* [52] can also potentially contribute to collagen metabolism. It is to highlight that there are a small number of microorganisms that can secrete both acids and collagenases, and that this study suggest that these microorganisms are enriched in bone-associated microbiomes where sulfur, and also nitrogen, polysaccharides and polypeptides biogeochemistry co-exists. Finally, biochemical knowledge for members of *Victivallaceae* and *Kiritimatiellae*, from which few cultured representatives are available [53,54], is limited; in this study, their capacity to presumptively degrade collagen, and α-mannose, α-fucose and β-galactose residues is suggested. Opposite, this study reinforces the carbohydrate-based fermentative lifestyle of members of *Anaerolineae*, *Clostridiaceae, Lentisphaeria*, *Paenibacillaceae, Planctomycetota,* and *Verrucomicrobiae*, which being enriched in key genes catalyzing the hydrolysis of multiple of polysaccharides are also common inhabitants of the gut.

Whether the differences in the number of enzymes produced by generalists (r-selected or copiotrophic) or specialist (k-selected or oligotrophic) can also be translated into biochemical differences, e.g., lower or higher affinity for substrates, will be further explored in the future.

3.3. Biochemical characterization of bone-degrading enzymes

In order to characterize the bone bioprocessing potential of the identified enzymes, a set of the 2,043 identified such proteins were selected (for details see Section 2.3). A total of 47 non-redundant and taxonomically diverse sequences most likely encoding full-length enzymes covering eight hydrolytic activities, were selected (Table S4): U32 and M9 collagenases (10), β-galactosidases (7), α-fucosidases (6), β-N-acetyl-hexosaminidases (6), sialidases (6), α-mannosidases (6), α-rhamnosidases (4), and α-galactosidases (2). They were assigned to multiple phylogenetic groups, namely, *Bacteroidota* (33), *Proteobacteria* (6), *Chloroflexota* (6), *Desulfobacterota* (1), and *Krumholzibacteriota* (1); the phylogeny of two sequences remained unclear. Maximum identity to homologous proteins in NCBI nr database ranged from 92.4 to 46.1% and query coverages from 100 to 58% (calculated using DIAMOND) (Table S4). Proteins were recombinantly produced in two vectors encoding affinity-tags (total number of 94 protein-encoding constructs). A set of 13 out of the 47 protein targets were found to be produced in soluble and active form when produced at 12–16 °C in *E. coli* (Table 2).

The proteins produced in soluble-active form were recovered from samples BB_{T0} (T0182, T0193, T0216, T0217, T0218, T0220, T0201, T0215, T0199), BB_{C0} (T0204), OB_{T0} (T0207 and T0209) and OB_{T1} (T0191), whose origin is detailed in Table 1. They do show closest match within *Bacteroidota* (9), *Proteobacteria* (3) and *Chloroflexota* (1), and covered eight families of hydrolytic activities (Figs. 2 and 3). Five of these enzymes were successfully expressed with an N-terminal his-tag (p1-vector: T0191, T0193, T0199, T0209, T0215), and eight with a C-terminal his-tag (p12-vector: T0182, T0201, T0204, T0207, T0216, T0217, T0218, T0220). This result shows the advantage of using a multi-construct strategy in enzyme discovery. According to signalP v5.0, all the proteins except for T0204 have predicted signal peptides for secretion to the extracellular medium. After expression and purification (purity > 98%), all thirteen enzymes were characterized to determine their optimal parameters for activity (Table 2, Fig. 2, Fig. 3, Table S5) and kinetic performances towards multiple substrates (Table 2). Their structures were also evaluated by homology modeling (Fig. 4, Table S6).

Characterization of collagenases. One collagenase, T0182, was successfully expressed. T0182 is a 1,112 amino acid (AA)-long polypeptide, with residues 85–616 encoding a peptidase family M9 domain structure. Two extra non-proteolytic domains were predicted: three Polycystic Kidney Disease (PKD) domains (from 624 to 995), and a pre-peptidase C-terminal domain (from 1,010 to 1,112) (Fig. 4). T0182 is 52% identical (in 67% of its sequence) to *Clostridium histolyticum* ColG collagenase (Protein Data Bank [PDB] code 2Y50; [56]), with which it shares similar domain architecture. However, T0182 contains a PKD domain, which is not found in ColG or any other homologues. T0182 showed proteolytic

Table 2
Kinetic parameters of bone-degrading enzymes.

Protein	Substrate	K_m (mM)[3]	V_{max} (U mg^{-1})[3]	k_{cat} (s^{-1})[3]	k_{cat}/K_m (mM^{-1} s^{-1})[3]
T0182	BODIPY-FL casein[1]	n.d.	125 ± 18[2]	n.d.	n.d.
	FALGPA	4.24 ± 0.1	n.d.	1.77 ± 0.30	0.42 ± 0.04
T0191	*p*NP-Neu5Ac	0.18 ± 0.03	6.35 ± 0.45	511.71 ± 32.71	2,955 ± 674
	3-Sialyllactose	0.031 ± 0.001	n.d.	921.5 ± 3.17	29,725 ± 15
	6-Sialyllactose	0.053 ± 0.001	n.d.	550.5 ± 15.16	10,386 ± 20
T0193	*p*NP-Neu5Ac	0.55 ± 0.17	4.79 ± 0.79	508.05 ± 35.85	1,044 ± 388
	3-Sialyllactose	0.082 ± 0.06	n.d.	294.2 ± 9.6	3,587 ± 16
	Neu5Ac-GM_2	0.735 ± 0.031	n.d.	48.09 ± 3.84	65.42 ± 5.30
	*p*NP-βNAGlu	6.17 ± 0.92	n.d.	53.40 ± 2.58	8.65 ± 1.53
	Acetylchitotetraose	0.062 ± 0.051	n.d.	47.54 ± 8.16	766.8 ± 16
	Acetylchitotriose	9.96 ± 0.74	n.d.	26.71 ± 0.97	2.68 ± 0.13
	Glycoprotein feutin[2]	n.d.	948.3 ± 18.46	n.d.	n.d.
T0216	*p*NP-NAβGlu	0.025 ± 0.006	3.33 ± 0.28	1,194 ± 2	47,811 ± 2,424
	*p*NP-NAβGal	2.78 ± 1.09	0.28 ± 0.05	36.35 ± 1.51	15.7 ± 6.7
	Glycoprotein feutin[2]	n.d.	0.14 ± 0.05	n.d.	n.d.
T0217	*p*NP-NAβGlu	0.028 ± 0.012	0.030 ± 0.004	9.88 ± 0.25	436.9 ± 19.2
T0218	*p*NP-NAβGlu	0.134 ± 0.015	121.5 ± 3.59	83,512 ± 3,179	633,820 ± 946
	*p*NP-NAβGal	0.326 ± 0.037	4.66 ± 0.12	2,191 ± 54	6,833 ± 96
	Glycoprotein feutin[2]	n.d.	7.80 ± 0.31	n.d.	n.d.
T0220	*p*NP-NAβGlu	0.042 ± 0.004	0.07 ± 0.002	23.37 ± 0.92	563.6 ± 75.6
	*p*NP-NAβGal	2.30 ± 0.17	0.03 ± 0.001	1.15 ± 0.03	0.5 ± 0.05
T0201	*p*NP-αGal	6.22 ± 0.93	10.44 ± 0.54	343.06 ± 10.39	56.67 ± 10.14
T0215	*p*NP-αGal	0.062 ± 0.008	0.12 ± 0.008	79.83 ± 3.71	1,317 ± 230
	*p*NP-βAPyr	3.30 ± 0.73	0.42 ± 0.04	21.53 ± 1.66	6.98 ± 2.05
	Galactose-α-1,3-galactose	0.048 ± 0.009	n.d.	98.51 ± 8.51	2,052 ± 95
	Globotriaosylceramide	0.096 ± 0.001	n.d.	72.01 ± 6.4	750.1 ± 64
	Globotriaosylsphingosine	0.058 ± 0.007	n.d.	93.45 ± 4.13	1,611 ± 50
T0199	*p*NP-αRham	1.08 ± 0.15	2.29 ± 0.11	1,542 ± 1308	1,473 ± 325
T0204	*p*NP-βMan	0.127 ± 0.036	12.1 ± 0.95	1,622 ± 82	14,090 ± 4,637
T0207	*p*NP-β-Fuc	0.0118 ± 0.003	1.92 ± 0.12	2,273 ± 31	206,615 ± 5,513
	*p*NP-βGal	0.199 ± 0.032	1.87 ± 0.07	1,222 ± 33	6,334 ± 1,186
	*p*NP-αAPyr	1.732 ± 0.461	9.13 ± 1.64	602.86 ± 34.62	380.7 ± 121.2
T0209	*p*NP-αFuc	30.53 ± 17.64	5.91 ± 2.52	136.4 ± 5.98	6.88 ± 4.17

[1] Values in Δfluorescence min^{-1}.
[2] Activity as μg sialic acid mg^{-1} feutin.
[3] For comparisons, all reactions were performed in 50 mM Britton and Robinson buffer, pH 7.0 and 30 °C.

activity against BODIPY-FL casein (Table 2), and retained more that 70% of its optimal activity at pH from 5.0 to 8.0 (Fig. 2) and temperatures from 5 to 30 °C (Fig. 3). The catalytic performance of T0182 was compared to that of ColG by using FALGPA, a typical synthetic collagenase substrate that Resemble the Gly-X-Pro pattern commonly often found in collagen sequence [57]. T0182 showed a catalytic efficiency (k_{cat}/K_m) value of 0.42 ± 0.04 $^{s-1}$ mM^{-1}, which is about 3.2-fold higher than that of ColG at 25 °C and pH 7 [57].

Characterization of sialidases. Two sialidases, T0191 and T0193, were successfully produced. T0191, a 533 AA-long polypeptide, is 42% identical (in 90% of its sequence) to the two-domain Family 33 Glycosyl Hydrolase (GH) 6MRX from *Bacteroides* (Fig. 4), which exhibits preference for red meat-associated carbohydrates [58]. T0193 is a 631 AA-long polypeptide, organized in three-domains (Fig. 4): i) residues 64–397 are 26% identical to family glycoside hydrolase GH33 *trans*-sialidase 4XE9 (*Streptococcus pneumoniae TIGR4*) ii) residues 405–463 are related to the chitobiase/β-hexosa minidase C-terminal domain from *Serratia marcescens* (13 % identity); and iii) residues 527–626 correspond to a PA14 domain, likely involved in binding. There is no sialidase with this domain-structure neither characterized nor crystallized. No significant similarity (e-value > 10) was found when comparing T0191 to T0193.

As shown in Table 2, T0191 was found to be highly active towards the model substrate *p*NP-Neu5Ac, and it was also capable of cleaving both 2,3′- and 2,6′-linked sialic acid in the trisaccharide substrate sialyllactose, which were the preferred substrates (e.g., up to 10-fold higher k_{cat}/K_m compared to substrate *p*NP-Neu5Ac). Sialidase T0193 hydrolyzed at 3-fold lower k_{cat}/K_m *p*NP-Neu5Ac, and 2-3′-linked sialic acid in the trisaccharide substrate 3-sialyllactose (8-fold lower k_{cat}/K_m), but not 2-3′-linked sialic acid in 6-sialyllactose. As this enzyme contains a chitobiase/β-hexosami nidase C-terminal domain (residues 405–463), the capacity of T0193 to degrade known β-hexosaminidase substrates, such as Neu5Ac-GM_2, Neu5Ac-GM_3, *p*NP-NAβGlu, *p*NP-NAβGal, chitin-like oligosaccharides such as acetylchitobiose, acetylchitotriose and acetylchitotetraose, as well as the glycoprotein fetuin, was also evaluated. As shown in Table 2, T0193 was capable of efficiently degrading acetylchitotetraose, *p*NP-NAβGlu and acetylchitotriose, in this order, as well as fetuin and the ganglioside Neu5Ac-GM_2 which contain a terminal N-acetyl-β-galactosamine and a negatively charged sialic acid moiety [59]. None of these substrates were hydrolyzed by T0191. The fact that T0193, but not T0191, hydrolyzed fetuin might be related to its high content in hexosamines (ca. 5.5%), which may be linked to T0193′s capacity to degrade β-N-acetylglucosamine (Table 2).

Determination of optimal parameters further showed that whereas T0191 retained 70% of maximal activity at pH 6.5–7.0 (Fig. 2) and temperatures from 30 to 40 °C (Fig. 3), T0193 was active at lower pH (4.5) and temperature (20–35 °C) values.

Characterization of β-N-acetyl-hexosaminidases. Four β-N-acetyl-hexosaminidases were successfully produced in soluble form, namely, T0216 (559 AA-long polypeptide), T0217 (399 AA-long

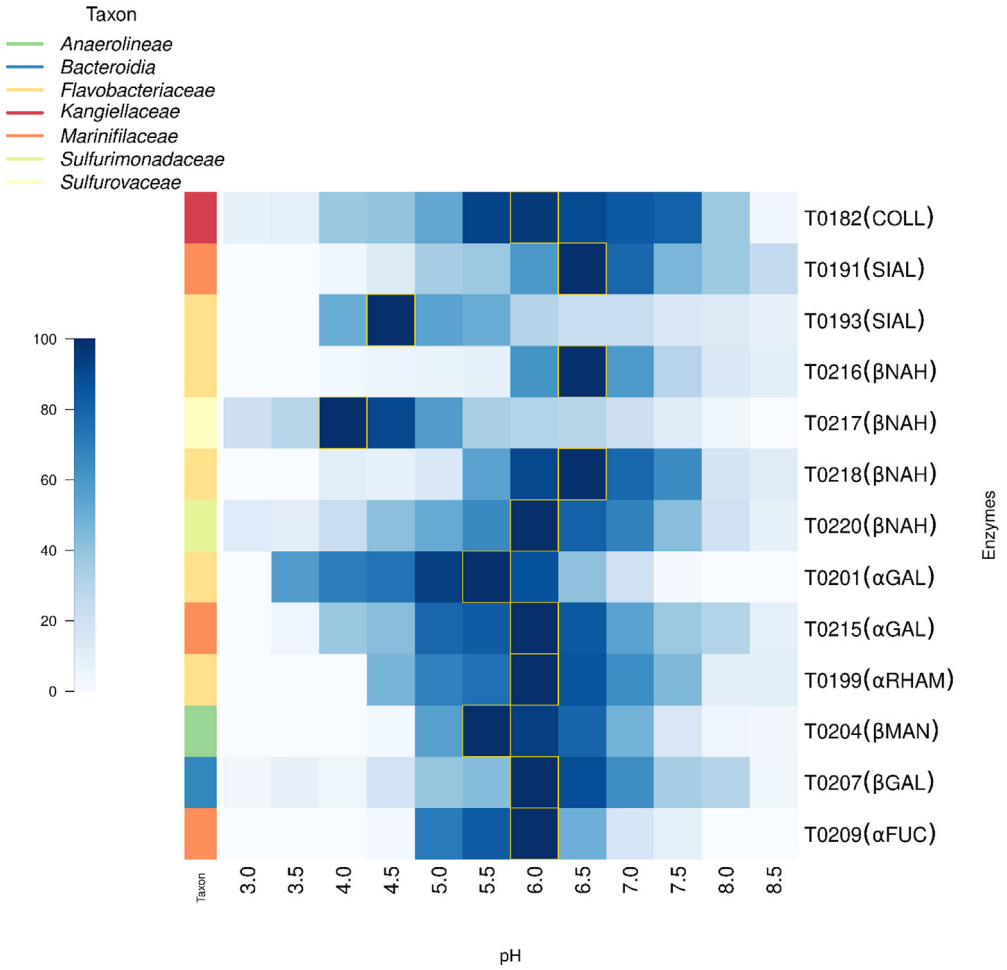

Fig. 2. Heatmap representing the pH profiles for the purified enzymes. Abbreviations as in Fig. 1. The data represent the relative percentages of specific activity, determined as follows: [protein], 0.002–0.04 mg ml^{-1}; [substrate], 0.3 mg ml^{-1}; pH, 3.0–9.0; T, 30 °C; reaction volume, 200 µl. The plot was made with heatmap3 R package version 1.9.1 [55]. The raw data are available in Table S5.

polypeptide), T0218 (995 AA-long polypeptide) and T0220 (558 AA-long polypeptide). These were 34.94, 33.78, 35.16, and 34.54 % identical (coverage: 93, 86, 84, and 89 %), respectively, to the GH3-NagZ catalytic domain of the N-acetylglucosaminidase 3BMX from *Bacillus subtilis* [60], although presenting different domain composition as is frequently encountered within the GH3 family (Fig. 4). Thus, the four enzymes contain at their N-terminal catalytic domains the Asp nucleophile and a conserved motif including the His/Asp dyad located in a flexible loop, which is characteristic of the GH3-NagZ subfamily. Pairwise identities range from 29.5% (T0216 vs T0217) to 49.9% (T0217 vs T0220). As shown in Table 2, T0218, T0220 and T0216 showed high activity towards *p*NP-NAβGlu, in this order from higher to lower activity, and to less extent towards *p*NP-NaβGal. This specificity differs to that of T0217, only capable of hydrolyzing *p*NP-NaβGlu, which was also the less catalytically efficient enzyme. T0218, and to lower extend T0216 (56-fold in terms of V_{max}) were also capable of hydrolyzing fetuin, which contain N-acetyl-β-glucosamine [59,61].

T0216 retained 70% of maximal activity at pH 6.5 and 5–40 °C, T0217 at pH 4.0–4.5 and 45–65 °C, T0218 at pH 6.0–7.0 and 20–35 °C, and T0220 at pH 6.0–7.0 and 40–45 °C (Figs. 2 and 3).

Characterization of α-galactosidases. Two α-N-galactosidases were successfully produced, namely, T0215 (403 AA-long polypeptide) and T0201 (404 AA-long polypeptide). They are both 43% identical to GH27 α-galactosidase 6F4C from *Nicotiana benthamiana* [62] (Fig. 4). Pairwise comparison revealed an identity of 39.8% between T0201 and T0215. As shown in Table 2, T0215 was active towards *p*NP-αGal and to lower extend *p*NP-βAPyr (188-fold lower k_{cat}/K_m). By contrast, T0201 was only able to cleave *p*NP-αGal, at 23-fold lower k_{cat}/K_m. Since glycoproteins in red meat and mature bone also tend to contain a high proportion of galactose, complex substrates containing such molecules were also tested. In this regard, we found that T0215 was also capable of degrading galactose-α-1,3-galactose, globotriaosylsphingosine and globotriaosylceramide, in this order. None of these substrates were hydrolyzed by T0201. This suggest T0215 is capable of cleaving terminal α-linked galactose residues from glycoconjugates.

T0215 retained 70% of maximal activity at pH 5.0–6.5 and 35–45 °C, whereas T0201 at pH 4.0–6.0 and 30–40 °C (Figs. 2 and 3).

Characterization of α-rhamnosidase. T0199, a 1,156 AA-long polypeptide, was the only α-rhamnosidase successfully produced. Residues 20–917 are 40% identical to GH78 α-rhamnosidase 6I60 from *Dictyoglomus thermophilum* [63] (Fig. 4). T0199 was found to be active towards *p*NP-αRham (Table 2), and retained 70% of maximal activity at pH 5.0–6.5 (Fig. 2), and 20–40 °C (Fig. 3).

Characterization of β-mannosidases. Only one β-mannosidase was successfully produced, T0204, a 890 AA-long polypeptide, 33% identical to β-mannosidase 2JE8 from *Bacteroides thetaiotaomicron* VPI-5482 [64]; it also showed low similarity to GH2 β-galactosidase 6ED1 (25%) and exo- β-D-glucosaminidase 2VZT from *Amycolatopsis orientalis* (21%) [65] (Fig. 4). T0204 was only

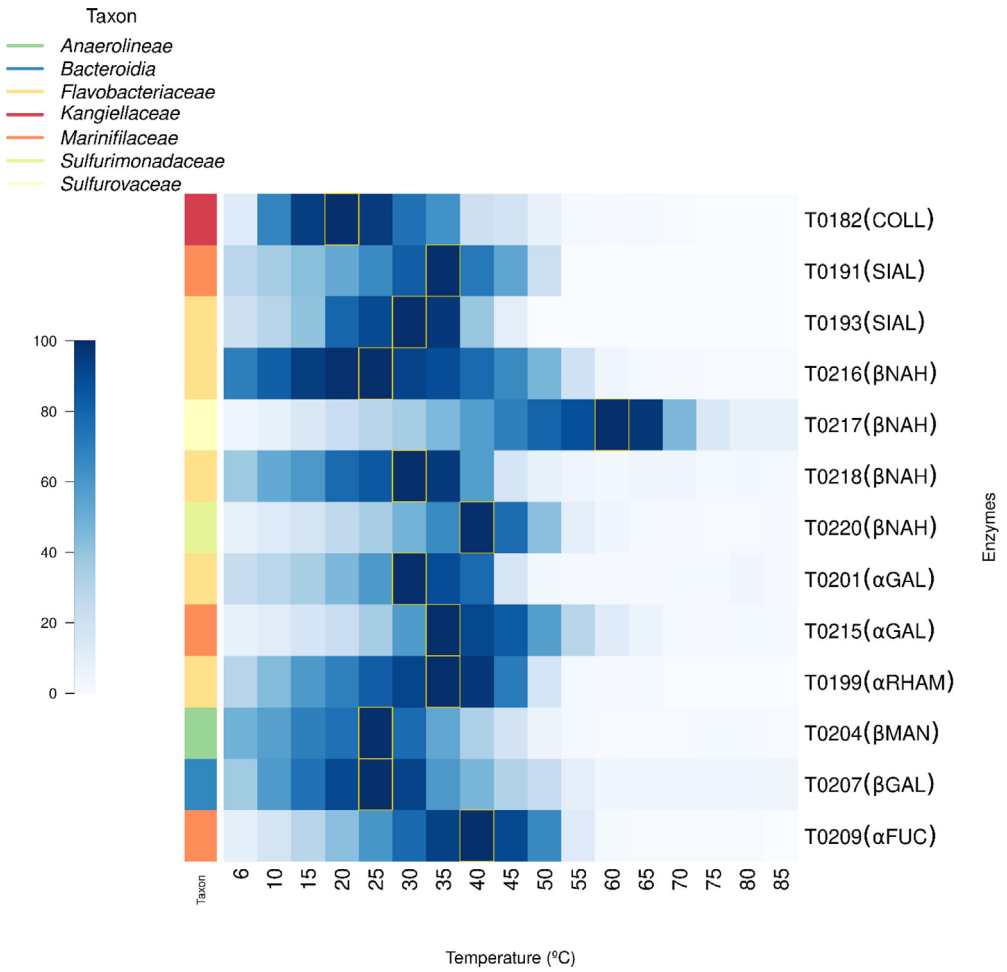

Fig. 3. Heatmap representing the temperature profiles for the purified enzymes. Abbreviations as in Fig. 1. The data represent the relative percentages of specific activity, determined in triplicate as follows: [protein], 0.002–0.04 mg ml^{-1}; [substrate], 0.3 mg ml^{-1}; pH 7.0; T, 5–80 °C; reaction volume, 200 μl. The plot was made with heatmap3 R package version 1.9.1 [55]. The raw data are available in Table S5.

capable of hydrolyzing *p*NP-βMan (Table 2) and retained 70% of maximal activity at pH 5.5–6.5 (Fig. 2) and temperatures ranging from 15 to 30 °C (Fig. 3).

Characterization of β-galactosidases. One β-galactosidase was successfully produced, T0207, a 820 AA-long polypeptide which is 39% identical to GH2 β-galactosidase 6B6L from *Bacteroides cellulosilyticus* (Fig. 4). T0207 showed activity against *p*NP-βFuc, *p*NP-βGal, and *p*NP-αAPyr, in this order (Table 2), and retained 70% of maximal activity at pH 6.0–6.5 (Fig. 2) and 15–30 °C (Fig. 3).

Characterization of α-fucosidases. T0209, a 836-long polypeptide, was the only α-fucosidase successfully produced. It contains an atypical domain structure (Fig. 4): i) residues 44–348 feature an undefined GH 43, 62 or 117-like domain (clan GH-F, with no clear activity assigned; and ii) residues 367–835 comprise a α-fucosidase domain. Most similar characterized homologue (41%) is α-fucosidase from *Thermotoga maritima* MSB8 (1ODU; [66]). T0209 was only found active against *p*NP-αFuc (Table 2), and retained 70% of maximal activity at pH 5.0–6.0 (Fig. 2) and 30–45 °C (Fig. 3).

3.4. The bone-degrading marine microbiomes contain biochemically versatile hydrolytic enzymes

The biochemical analyses presented in Section 3.3 demonstrate that some of the recovered enzymes, e.g., sialidases T0191 and T0193, α-galactosidase T0215 and β-N-acetylhexosaminidase T0216 from *Flavobacteriaceae* and *Marinifilaceae* (*Bacteroidota* phylum), showed high performances for the degradation of complex glycoproteins present in mature bones (Table 2) at a broad range of pH (Fig. 2) and temperature (Fig. 3) values. Remarkably, results also revealed that enzymes from bone-degrading microbiomes optimally work at different temperature ranges, e.g., those assigned to *Kangiellaceae* (*Proteobacteria* phylum) were most active at temperatures from 5 to 30 °C, whereas those assigned to *Flavobacteriaceae* (*Bacteroidota* phylum) and *Anaerolineae* (*Chloroflexota* phylum) were so at temperatures from 15 to 40 °C, and those assigned to *Marinifilaceae* (*Bacteroidota* phylum) had a slightly higher but narrower temperature range (30–45 °C). Finally, those assigned to *Sulfurovaceae* and *Sulfurimonadaceae* (*Campylobacterota* phylum) showed the highest temperature range, as high as 40–65 °C. These variations in thermal profiles contrast with the *in situ* temperatures at the sampling site, which range from 4 to 6 °C [27], and with the fact that all but one (T0204) of the enzymes have a predicted leader sequence for secretion. These differences were also observed at the level of substrate range, which was broader for enzymes from *Flavobacteriaceae* (e.g., T0193 and T0216) and *Marinifilaceae* (e.g., T0191 and T0215) compared to similar microbial counterparts (see Table 2). This profile diversity indicates that a community effort is needed to degrade bones [27] with each microorganism hosting and contributing to different families of target collagenases and glycosidases, but also that each microbial member harbours distinct activity profiles.

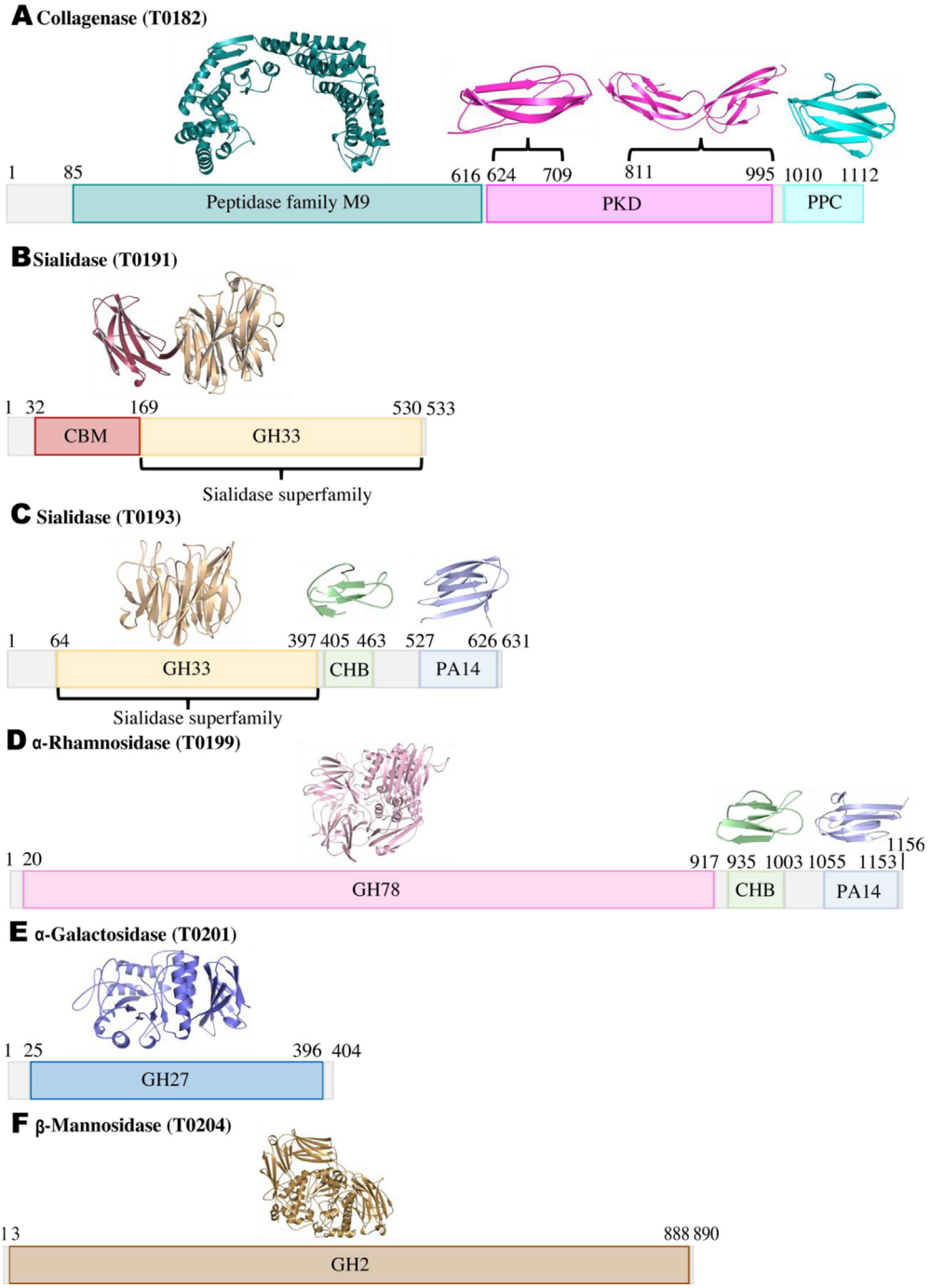

Fig. 4. (a) Domain structure for the purified enzymes defined by BLAST, and modelled by Swissmodel and Phyre2. PDB codes used as templates are shown in Table S6. (b) Domain structure for the purified enzymes defined by BLAST, and modelled by Swissmodel and Phyre2. PDB codes used as templates are shown in Table S6.

The results also suggest that members of *Flavobacteriaceae* and *Marinifilaceae*, which contribute to 22% of all the hydrolytic enzymes studied (hosting 9 out 10 hydrolytic families herein targeted) (Table S7), may represent a promising starting point for the development of enzyme cocktails to degrade complex and recalcitrant protein-rich residues, such as bones. Moreover, some of the enzymes did show novelty at the sequence and domain architecture level. Thus, whereas seven enzymes were 30–50 % identical in all their sequences to proteins deposited in the PDB, five (T0193, T0199, T0209, T0218 and T0220) were 25–40 % identical only partially to structurally homologous proteins. However, the sequence databases contain proteins with the same domain architecture to all these five. On the other hand, collagenase T0182 seems unique in that the closest reported sequences lack one PKD repeat.

3.5. Multi-enzyme formulations from marine bone microbiomes allow bone meal degradation in vitro

Chromogenic bone meal (see Section 2.6) was used to evaluate the potential of a multi-enzymatic cocktail for degrading recalcitrant deboning residues. Collagenase T0182 was used alone or in combination with a cocktail of the best performing glycohydrolytic enzymes in terms of catalytic efficiency and broader substrate

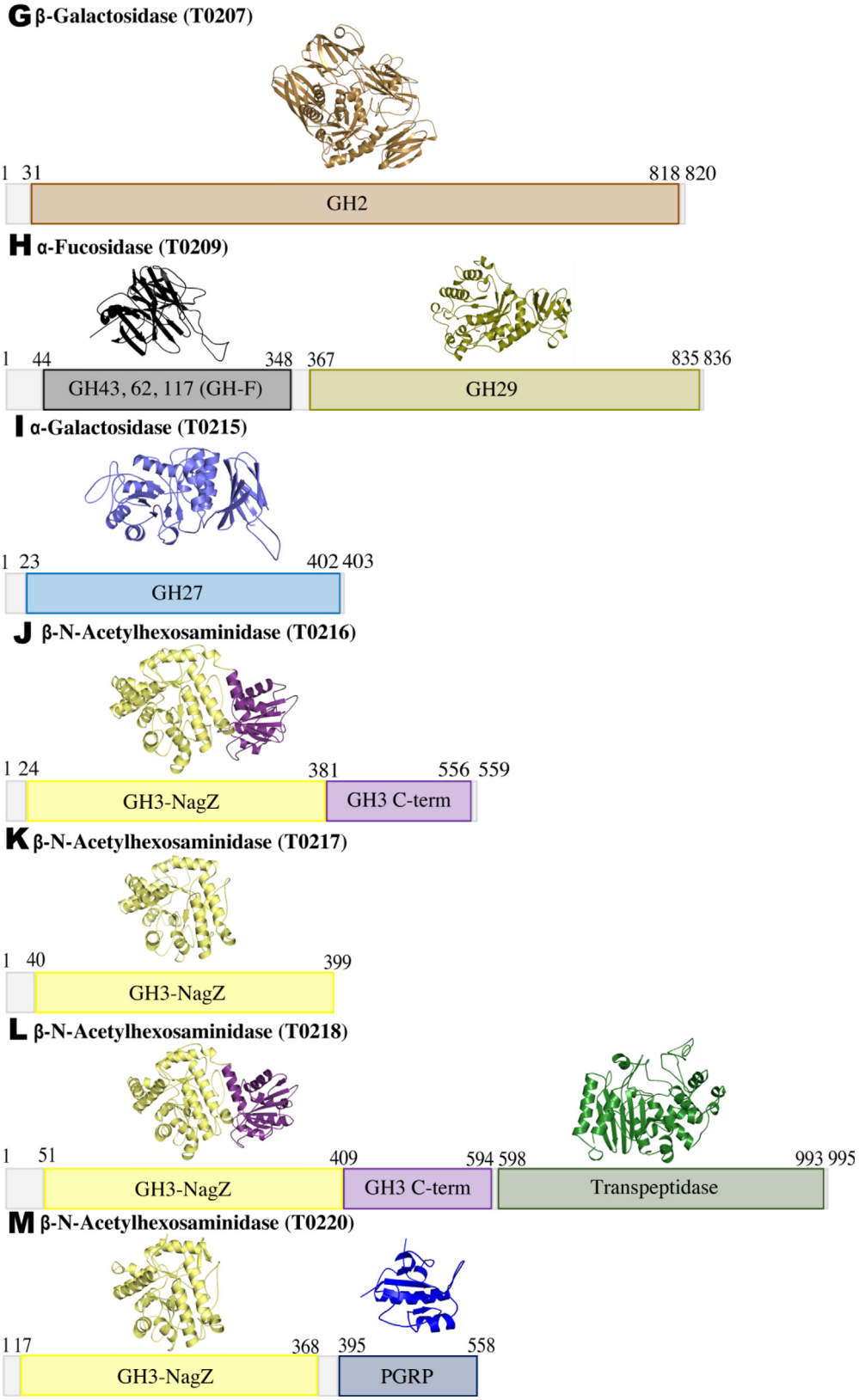

Fig. 4 (*continued*)

range (Table 2). The glycohydrolytic *cocktail* included enzymes covering seven different families, namely, T0193 (sialidase), T0199 (α-rhamnosidase), T0204 (β-mannosidase), T0207 (β-galactosidase), T0209 (α-fucosidase), T0215 (α-galactosidase), and T0216 (β-N-acetylhexosaminidase). As shown in Table 3, when collagenase T0182 was assayed alone with the bone meal at pH 7.0 and 30 °C, the signal was almost 21 times higher than the background. In addition, in the absence of T0182 collagenase, the glyco-

Table 3
Bone-meal degradation tests.

Sample[1]	Δabsorbance (a.u.) per min
Control	0.325 ± 0.027
T0182	6.800 ± 0.212
Glycohydrolytic *cocktail*	0.341 ± 0.011
T0182 + glycohydrolytic *cocktail*	15.498 ± 0.37

[1] Shown is the Δabsorbance at 517 nm per min, determined as follows: [protein], 1 mg; pH, 50 mM Britton and Robinson buffer pH 7.0; T, 30 °C; reaction volume, 200 μl; reaction time, 20 min.

hydrolytic *cocktail* did not render any significant activity towards the bone-meal substrate, with absorbance values similar to background. Interestingly, the activity was approximately 48 times higher than the background when T0182 was combined with the glycohydrolytic *cocktail*.

Degradation tests were also performed using demineralized chicken thigh bone (Section 2.7), as another model substrate. The bones were acid-treated and then extensively and manually cleaned to remove cellular remnants and non-collagenous proteins at the surface, before they were freeze-dried. Then, 1% (w/v) lyophilized acid-treated bone material (Fig. S1) was incubated at pH 7.0 and 30 °C, in the presence of enzymatic materials (see Table 3), and the reaction products were analyzed after 72 h incubations by HPAEC-PAD. After 72 h, no reaction products were observed in the control reaction nor in the presence of the glycohydrolytic *cocktail* (Fig. 5). However, degradation products were clearly observed in the presence of the collagenase T0182. Moreover, the product profile when T0182 and the *cocktail* were combined, significantly differs from that in the presence of T0182 alone. We hypothesized that differences were due to the formation of peptides with different degree of glycosylations, which was later confirmed by quantifying the reducing sugars released by the DNS method. Indeed, the reducing sugars in the 72 h samples containing either the control (no enzyme), the glycohydrolytic *cocktail* or the collagenase T0182 samples were below detection limit. However, when T0182 was combined with the glycohydrolytic *cocktail*, reducing sugars reached 11.4 ± 0.1 μg mg $^{-1}$ of bone material.

Although the assay conditions (incubation time, enzyme to bone material ratio, pH, temperature, etc.) and the enzymes conforming the cocktail have not been optimized and the nature of the degradation products remains to be determined, these results demonstrate that the combined use of enzymes retrieved from bone-degrading microbiomes, particularly, through the integration of glycosidic and collagenolytic hydrolases, significantly promotes the degradation of bone material. A suitable design of enzyme cocktails and careful selection of the assay conditions may allow the development of industrial processes for the efficient hydrolysis of recalcitrant protein-rich materials.

4. Conclusions

The microbial diversity of bone-degrading microbiomes and the synergistic mechanisms by which their enzymes degrade bones are beginning to be understood. Our goal was to accumulate data on the characteristics of the enzymes in bone-degrading microbiomes and to evaluate their versatility and biotechnological potential, for which little is known to date. By using a multi-disciplinary approach, combining bone-degradation field experiments, sequencing, bioinformatics, three-dimensional modeling, gene synthesis and expression, activity and bone deployment assessments, we were able to recover 2,043 taxonomically and functionally diverse hydrolytic enzymes presumptively degrading bone material components, and to report the characteristics of thirteen

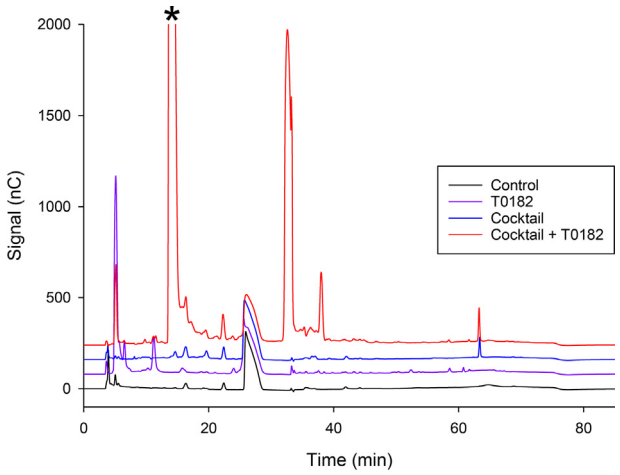

Fig. 5. Representative HPAEC-PAD chromatograms of the reaction products when chicken thigh demineralized bone was enzymatically treated during 72 h. Reaction conditions: [bone material]: 1% (w/v) in 480 μl of 50 mM Britton and Robinson buffer, pH 7.0; [protein]: 20 μl of the enzyme solutions (10 mg ml^{-1}); Temperature: 30 °C; Incubation time: 72 h. Samples were as in Table 3. The peak at 25–28 min corresponds to buffer. The peaks detected in sample T0182 are likely collagenolytic short peptides. The peaks detected in samples where the glycohydrolytic *cocktail* was mixed with T0182 might correspond to collagenolytic short peptides and/or oligosaccharides. The nature of these reaction products remains to be further evaluated. Note: the asterisk indicated a peak that most likely represent a monosaccharide (e.g., galactose or glucose, but not xylose) based on the elution compared to standards.

of them. The main outcomes of our combined analyses conducted in this study are I) that only members of *Bacteroidota* produce all enzymes capable of degrading complex sialo/glycoproteins present in mature bones, with the rest of microbial members being specialists; II) that enzymes are highly versatile, acting against a broad range of sialo/glyco-proteins at a broad range of pH and temperatures, a feature that can contribute to a high environmental plasticity of bone-degrading marine microbiomes (e.g., degradation of multiple types of bones under multiple conditions); and III) that enzymes, particularly those from *Flavobacteriaceae* and *Marinifilaceae*, not only play a major role in the bone degradation *in vivo*, but also represent a promising starting point for the development of cocktails to degrade recalcitrant protein-rich deboning residues.

It is worth mentioning that the purposes of this research is not to elucidate the precise action of collagenases and other glycosidases, nor to investigate mineralisation of collagen and complex carbohydrates that constitute bones. Rather, to evaluate and utilise bone-associated microbiomes as potential biological resource for such enzymes and to evaluate their use for the valorisation of bone residues in the biorefinery industry. Extending the analysis carried out in this study to a larger number of enzymes and optimizing the design of enzyme cocktails and the bone degradation process will help to gain a deeper insight into the real potential of bone-degrading marine microbiomes in the biorefinery industry. Our knowledge base on which microorganisms and enzymes are most versatile will help in the process of selecting and evaluating of such new enzymes. The limitations of the present work in terms of understanding the degradation of hydroxyapatite-polypeptides (collagen)-polysaccharide networks at the molecular level, will further benefit from a deeper structural and biochemical analysis of the enzymes herein identified. Other limitation is that some of the specialized phyla suggested to play a role in bone degradation may not contribute *in vivo* to bone degradation, since their hydrolytic enzymes are too distantly related to assume isofunctions. Extending the characterization efforts to other sets of distantly related enzymes herein identified may help clarifying this.

CRediT authorship contribution statement

Laura Fernandez-Lopez: Methodology, Formal analysis. **Sergio Sanchez-Carrillo:** Formal analysis. **Antonio García-Moyano:** Methodology, Resources. **Erik Borchert:** Methodology, Formal analysis. **David Almendral:** Methodology. **Sandra Alonso:** Methodology, Formal analysis. **Isabel Cea-Rama:** Methodology, Formal analysis. **Noa Miguez:** Methodology, Formal analysis. **Øivind Larsen:** Methodology. **Johannes Werner:** Formal analysis. **Kira S. Makarova:** Methodology. **Francisco J. Plou:** Methodology, Funding acquisition. **Thomas G. Dahlgren:** Methodology. **Julia Sanz-Aparicio:** Formal analysis, Funding acquisition. **Ute Hentschel:** Methodology, Resources, Funding acquisition. **Gro Elin Kjæreng Bjerga:** Methodology, Formal analysis, Resources, Funding acquisition. **Manuel Ferrer:** Formal analysis, Funding acquisition, Resources, Writing – original draft, Writing – review & editing.

Declaration of Competing Interest

The authors declare that they have no known competing financial interests or personal relationships that could have appeared to influence the work reported in this paper.

Acknowledgments

We acknowledge financial support of ERA-NET Marine Biotechnology (GA no.: 604814) funded under the FP7 ERA-NET scheme and nationally managed from the German Federal Ministry of Education and Research and Norwegian Research Council, the grants PCIN-2017-078 (within the Marine Biotechnology ERA-NET), BIO2017-85522-R, PID2020-112758RB-I00 and PDC2021-121534-I00 from the Ministerio de Economía, Industria y Competitividad, Ministerio de Ciencia e Innovación, Agencia Estatal de Investigación (AEI) (Digital Object Identifier 10.13039/501100011033), Fondo Europeo de Desarrollo Regional (FEDER) and the European Union (“NextGenerationEU/PRTR”), and the grant 2020AEP061 from the Agencia Estatal CSIC. F.J.P and J.S-A. acknowledges grants PID2019-105838RB-C31 and PID2019-105838RB-C33 from the Ministerio de Ciencia e Innovación, Agencia Estatal de Investigación (AEI), Fondo Europeo de Desarrollo Regional (FEDER) and the European Union (EU). Additional funding was received from the Norwegian Biodiversity Information Centre (PA 809116 knr. 47-14) and NORCE Norwegian Research Centre. J.W. acknowledge the use of de.NBI cloud and the support by the High Performance and Cloud Computing Group at the Zentrum für Datenverarbeitung of the Eberhard Karls University of Tübingen and the Federal Ministry of Education and Research (BMBF) through grant no 031 A535A. K.S.M. is supported by intramural funds of the US Department of Health and Human Services (to the National Library of Medicine).

We thank Hans T. Kleivdal for early developments of the concept. We thank Norilia AS for supplying bone residue material for the field work and ROV AS for providing underwater services during the deployment and sampling campaign.

Appendix A. Supplementary data

Supplementary data to this article can be found online at https://doi.org/10.1016/j.csbj.2021.11.027.

References

[1] Saitta ET, Liang R, Lau MC, Brown CM, Longrich NR, Kaye TG, et al. Cretaceous dinosaur bone contains recent organic material and provides an environment conducive to microbial communities. Elife 2019;8:e46205.
[2] Kontopoulos I, Penkman K, Mullin VE, Winkelbach L, Unterländer M, Scheu A, et al. Screening archaeological bone for palaeogenetic and palaeoproteomic studies. PLoS ONE 2020;15:e0235146.
[3] Quach D, Collins F, Parameswaran N, McCabe L, Britton RA, Ellermeier CD, et al. Microbiota reconstitution does not cause bone loss in germ-free mice. mSphere 2018;3. e00545-17.
[4] Steffen W, Richardson K, Rockström J, Cornell SE, Fetzer I, Bennett EM, et al. Sustainability. Planetary boundaries: Guiding human development on a changing planet. Science 2015;347:6223.
[5] Shukla PR, Skea J, Calvo Buendia E, Masson-Delmotte V, Pörtner HO, Roberts DC, et al. IPCC, 2019: Climate Change and Land: an IPCC special report on climate change, desertification, land degradation, sustainable land management, food security, and greenhouse gas fluxes in terrestrial ecosystems. 2019
[6] Lasekan A, Abu Bakar F, Hashim D. Potential of chicken by-products as sources of useful biological resources. Waste Manag 2013;33:552–65.
[7] Gómez-Guillén MC, Giménez B, López-Caballero ME, Montero MP. Functional and bioactive properties of collagen and gelatin from alternative sources: A review. Food Hydrocoll 2011;25:1813–27.
[8] FAO. FAOSTAT. Food and Agriculture Organization of the United Nations, 2012.
[9] Kuboki Y, Watanabe T, Tazaki M, Taktta H. Comparative biochemistry of bone matrix proteins in bovine and fish. In: Suga S, Nakahara H, editors. Mechanisms and phylogeny of mineralization in biological systems. Tokyo, Japan: Springer; 1991. p. 495–9.
[10] Robey P. Bone matrix proteoglycans and glycoproteins. In: Bilezikian J, Raisz L, Rodan G, editors. Principles of bone biology. New York, NY: Elsevier; 2002. p. 225–37.
[11] Sato S, Rahemtulla F, Prince CW, Tomana M, Butler WT. Acidic glycoproteins from bovine compact bone. Connect Tissue Res 1985;14:51–64.
[12] Shoulders MD, Raines RT. Collagen structure and stability. Annu Rev Biochem 2009;78:929–58.
[13] Tresguerres M, Katz S, Rouse GW. How to get into bones: proton pump and carbonic anhydrase in *Osedax* boneworms. Proc Biol Sci 2013;280:20130625.
[14] Deming JW, Reysenbach A-L, Macko SA, Smith CR. Evidence for the microbial basis of a chemoautotrophic invertebrate community at a whale fall on the deep seafloor: bone-colonizing bacteria and invertebrate endosymbionts. Microsc Res Technol 1997;37:162–70.
[15] Rouse GW, Goffredi SK, Vrijenhoek RC. *Osedax*: Bone-eating marine worms with dwarf males. Science 2004;305:668–71.
[16] Glover AG, Källström B, Smith CR, Dahlgren TG. World-wide whale worms? A new species of *Osedax* from the shallow north Atlantic. Proc Biol Sci 2005;272:2587–92.
[17] Goffredi SK, Orphan VJ, Rouse GW, Jahnke L, Embaye T, Turk K, et al. Evolutionary innovation: a bone-eating marine symbiosis. Environ Microbiol 2005;7:1369–78.
[18] Dahlgren T, Wiklund H, Källström B, Lundälv T, Smith C, Glover A. A shallow-water whale-fall experiment in the North Atlantic. Cah Biol Mar 2006;47: 385-9.
[19] Goffredi SK, Johnson SB, Vrijenhoek RC. Genetic diversity and potential function of microbial symbionts associated with newly discovered species of *Osedax polychaete* worms. Appl Environ Microbiol 2007;73:2314–23.
[20] Verna C, Ramette A, Wiklund H, Dahlgren TG, Glover AG, Gaill F, Dubilier N. High symbiont diversity in the bone-eating worm *Osedax mucofloris* from shallow whale-falls in the North Atlantic. Environ Microbiol. 2010;12: 2355-70.
[21] Vietti LA, Bailey JV, Ricci EM. Insights into the microbial degradation of bone in marine environments from rRNA gene sequencing of biofilms on lab-simulated carcass-falls. Spec Publ (Paleontol Soc) 2014;13:120–1.
[22] Aronson HS, Zellmer AJ, Goffredi SK. The specific and exclusive microbiome of the deep-sea bone-eating snail, *Rubyspira osteovora*. FEMS Microbiol Ecol 2017;93:fiw250.
[23] Miyamoto N, Yoshida MA, Koga H, Fujiwara Y. Genetic mechanisms of bone digestion and nutrient absorption in the bone-eating worm *Osedax japonicus* inferred from transcriptome and gene expression analyses. BMC Evol Biol 2017;17:17.
[24] Rouse GREGW, Goffredi SHANAK, Johnson SHANNONB, Vrijenhoek ROBERTC. An inordinate fondness for *Osedax* (Siboglinidae: Annelida): Fourteen new species of bone worms from California. Zootaxa 2018;4377:451–89.
[25] Eriksen AMH, Nielsen TK, Matthiesen H, Carøe C, Hansen LH, Gregory DJ, et al. Bone biodeterioration-The effect of marine and terrestrial depositional environments on early diagenesis and bone bacterial community. PLoS ONE 2020;15:e0240512.
[26] Hewitt OH, Díez-Vives C, Taboada S. Microbial insights from Antarctic and Mediterranean shallow-water bone-eating worms. Polar Biol 2020;43:1605–21.
[27] Borchert E, García-Moyano A, Sanchez-Carrillo S, Dahlgren TG, Slaby BM, Bjerga GEK, et al. Deciphering a marine bone-degrading microbiome reveals a complex community effort. mSystems 2021;6. e01218-1220.
[28] Freitas RC, Marques HIF, Silva MACD, Cavalett A, Odisi EJ, Silva BLD, et al. Evidence of selective pressure in whale fall microbiome proteins and its potential application to industry. Mar Genomics 2019;45:21–7.
[29] Higgs ND, Glover AG, Dahlgren TG, Little CTS. Bone-boring worms: characterizing the morphology, rate, and method of bioerosion by *Osedax mucofloris* (Annelida, Siboglinidae). Biol Bull 2011;221:307–16.
[30] Goffredi SK, Yi H, Zhang Q, Klann JE, Struve IA, Vrijenhoek RC, et al. Genomic versatility and functional variation between two dominant heterotrophic symbionts of deep-sea *Osedax* worms. ISME J 2014;8:908–24.

[31] Buchfink B, Xie C, Huson DH. Fast and sensitive protein alignment using DIAMOND. Nat Methods 2015;12:59–60.
[32] Larkin MA, Blackshields G, Brown NP, Chenna R, McGettigan PA, McWilliam H, et al. Clustal W and Clustal X version 2.0. Bioinformatics 2007;23:2947–8.
[33] Eddy SR, Pearson WR. Accelerated profile HMM searches. PLoS Comput Biol 2011;7:e1002195.
[34] Dong X, Strous M. An integrated pipeline for annotation and visualization of metagenomic contigs. Front Genet 2019;10:999.
[35] Li W, Godzik A. Cd-hit: a fast program for clustering and comparing large sets of protein or nucleotide sequences. Bioinformatics 2006;22:1658–9.
[36] Boratyn GM, Schäffer AA, Agarwala R, Altschul SF, Lipman DJ, Madden TL. Domain enhanced lookup time accelerated BLAST. Biol Direct. 2012;7:12.
[37] Waterhouse A, Bertoni M, Bienert S, Studer G, Tauriello G, Gumienny R, et al. SWISS-MODEL: homology modelling of protein structures and complexes. Nucleic Acids Res. 2018;46 (W1): 296-303.
[38] Kelley LA, Mezulis S, Yates CM, Wass MN, Sternberg MJE. The Phyre2 web portal for protein modeling, prediction and analysis. Nature Protoc 2015;10:845–58.
[39] Geertsma ER, Dutzler R. A versatile and efficient high-throughput cloning tool for structural biology. Biochemistry 2011;50:3272–8.
[40] Bjerga GEK, Arsın H, Larsen Ø, Puntervoll P, Kleivdal HT. A rapid solubility-optimized screening procedure for recombinant subtilisins in *E. coli*. J Biotechnol 2016;222:38–46.
[41] Coscolín C, Katzke N, García-Moyano A, Navarro-Fernández J, Almendral D, Martínez-Martínez M, et al. Bioprospecting reveals class III ω-transaminases converting bulky ketones and environmentally relevant polyamines. Appl Environ Microbiol 2019;85. e02404-18.
[42] Placido A, Hai T, Ferrer M, Chernikova TN, Distaso M, Armstrong D, et al. Diversity of hydrolases from hydrothermal vent sediments of the Levante Bay, Vulcano Island (Aeolian archipelago) identified by activity-based metagenomics and biochemical characterization of new esterases and an arabinopyranosidase. Appl Microbiol Biotechnol 2015;99:10031–46.
[43] Thompson VF, Saldaña S, Cong J, Goll DE. A BODIPY fluorescent microplate assay for measuring activity of calpains and other proteases. Anal Biochem 2000;279:170–8.
[44] Lee JH, Song Y-A, Tannenbaum SR, Han J. Increase of reaction rate and sensitivity of low-abundance enzyme assay using micro/nanofluidic preconcentration chip. Anal Chem 2008;80:3198–204.
[45] Kračun SK, Schückel J, Westereng B, Thygesen LG, Monrad RN, Eijsink VGH, et al. A new generation of versatile chromogenic substrates for high-throughput analysis of biomass-degrading enzymes. Biotechnol Biofuels 2015;8:70.
[46] Talens-Perales D, Sánchez-Torres P, Marín-Navarro J, Polaina J. In silico screening and experimental analysis of family GH11 xylanases for applications under conditions of alkaline pH and high temperature. Biotechnol Biofuels 2020;3:198.
[47] Garcia-Gonzalez M, Plou FJ, Cervantes FV, Remacha M, Poveda A, Jiménez-Barbero J, et al. Efficient production of isomelezitose by a glucosyltransferase activity in Metschnikowia reukaufii cell extracts. Microb Biotechnol 2019;12:1274–85.
[48] Taboada S, Bas M, Avila C, Riesgo A. Phylogenetic characterization of marine microbial biofilms associated with mammal bones in temperate and polar areas. Mar Biodivers 2020;50:60.
[49] R Core Team. R version 3.6.3: A language and environment for statistical computing. R foundation for statistical computing, Vienna, Austria. https://www.R-project.org/. (2020).
[50] Warnes GR, Bolker B, Bonebakker L, Gentleman R, Huber W, Liaw A, et al. gplots: Various R Programming Tools for Plotting Data. R package version 3.1.1. https://CRAN.R-project.org/package=gplots. 2020.
[51] Duarte AS, Correia A, Esteves AC. Bacterial collagenases - A review. Crit Rev Microbiol 2016;42:106–26.
[52] Mori JF, Chen L-X, Jessen GL, Rudderham SB, McBeth JM, Lindsay MBJ, et al. Putative mixotrophic nitrifying-denitrifying gammaproteobacteria implicated in nitrogen cycling within the ammonia/oxygen transition zone of an oil sands pit lake. Front Microbiol 2019;10:2435.
[53] Colombino E, Biasato I, Ferrocino I, Bellezza Oddon S, Caimi C, Gariglio M, et al. Effect of insect live larvae as environmental enrichment on poultry gut health: gut mucin composition, microbiota and local immune response evaluation. Animals (Basel) 2021;11:2819.
[54] Spring S, Bunk B, Spröer C, Schumann P, Rohde M, Tindall BJ, et al. Characterization of the first cultured representative of *Verrucomicrobia* subdivision 5 indicates the proposal of a novel phylum. ISME J 2016;10:2801–16.
[55] Zhao S, Yin L, Guo Y, Sheng Q, Shyr Y. heatmap3: An Improved heatmap package. R package version 1.1.9. https://CRAN.R-project.org/package=heatmap3. 2021.
[56] Eckhard U, Schönauer E, Nüss D, Brandstetter H. Structure of collagenase G reveals a chew-and-digest mechanism of bacterial collagenolysis. Nat Struct Mol Biol 2011;18:1109–14.
[57] Eckhard U, Schönauer E, Ducka P, Briza P, Nüss D, Brandstetter H. Biochemical characterization of the catalytic domains of three different Clostridial collagenases. Biol Chem 2009;390:11–8.
[58] Zaramela LS, Martino C, Alisson-Silva F, Rees SD, Diaz SL, Chuzel L, et al. Gut bacteria responding to dietary change encode sialidases that exhibit preference for red meat-associated carbohydrates. Nat Microbiol 2019;4:2082–9.
[59] Spiro RG. Studies on fetuin, a glycoprotein of fetal serum. I. Isolation, chemical composition and physiocochemical properties. J Biol Chem 1960;235:2860–9.
[60] Litzinger S, Fischer S, Polzer P, Diederichs K, Welte W, Mayer C. Structural and kinetic analysis of *Bacillus subtilis* N-acetylglucosaminidase reveals a unique Asp-His dyad mechanism. J Biol Chem 2010;285:35675–84.
[61] Bosmann HB. Glycoproteins biosynthesis: purification and properties of glycoproteins. EWur J Biochem 1970;14:33–40.
[62] Kytidou K, Beekwilder J, Artola M, van Meel E, Wilbers RHP, Moolenaar GF, et al. *Nicotiana benthamiana* α-galactosidase A1.1 can functionally complement human α-galactosidase A deficiency associated with Fabry disease. J Biol Chem 2018;293:10042–58.
[63] Guillotin L, Kim H, Traore Y, Moreau P, Lafite P, Coquoin V, et al. Biochemical characterization of the α-l-rhamnosidase DtRha from *Dictyoglomus thermophilum*: Application to the selective derhamnosylation of natural flavonoids. ACS Omega 2019;4:1916–22.
[64] Tailford LE, Money VA, Smith NL, Dumon C, Davies GJ, Gilbert HJ. Mannose foraging by *Bacteroides thetaiotaomicron*: structure and specificity of the beta-mannosidase, BtMan2A. J Biol Chem 2007;282:11291–9.
[65] Biernat KA, Pellock SJ, Bhatt AP, Bivins MM, Walton WG, Tran BNT, et al. Structure, function, and inhibition of drug reactivating human gut microbial β-glucuronidases. Sci Rep 2019;9:825.
[66] Sulzenbacher G, Bignon C, Nishimura T, Tarling CA, Withers SG, Henrissat B, et al. Insights into the catalytic mechanism and the molecular basis for fucosidosis. J Biol Chem 2004;279:13119–28.